



CHALMERS
UNIVERSITY OF TECHNOLOGY



Energy-Optimal Platooning with Hybrid Vehicles

Mattias Hovgard
Oscar Jonsson

MASTER'S THESIS EX028/2017

Energy-Optimal Platooning with Hybrid Vehicles

MATTIAS HOVGARD
OSCAR JONSSON



CHALMERS
UNIVERSITY OF TECHNOLOGY

Department of Electrical Engineering
CHALMERS UNIVERSITY OF TECHNOLOGY
Gothenburg, Sweden 2016

Energy-Optimal Platooning with Hybrid Vehicles
MATTIAS HOVGARD, OSCAR JONSSON

© MATTIAS HOVGARD, OSCAR JONSSON, 2017.

Supervisor: Nikolce Murgovski, Department of Electrical Engineering
Jonas Fredriksson, Department of Electrical Engineering
Martin Sanfridsson, Volvo Group
Examiner: Nikolce Murgovski, Department of Electrical Engineering

Master's Thesis EX028/2017
Department of Electrical Engineering
Chalmers University of Technology
SE-412 96 Gothenburg
Telephone +46 31 772 1000

Cover: A Volvo hybrid concept truck [1].

Typeset in L^AT_EX
Gothenburg, Sweden 2017

Energy-Optimal Platooning with Hybrid Vehicles
MATTIAS HOVGARD, OSCAR JONSSON
Department of Electrical Engineering
Chalmers University of Technology

Abstract

The objective of this master thesis is to present a control strategy capable of minimizing the fuel consumption of hybrid electric vehicles traveling in a platoon on a road with a known topography. The main idea is to minimize the amount of energy that is wasted because of the air resistance and by braking with the mechanical brakes. The former is achieved by having the vehicles drive close after one another. The latter can be achieved by either allowing the speed to vary and thereby avoid braking altogether, or by using the electric machine to brake and storing the kinetic energy of the vehicle as electric energy in the battery. The control strategy finds the optimal states: velocity, battery state of charge, travel time, gear and engine state. It also finds the optimal control signals: the force from the engine, electric machine and mechanical brakes as well as switching gear and changing engine state. To make it less computationally demanding the optimization formulation is divided into two layers. One that finds the optimal velocity, battery state of charge and travel time using convex optimization and one that finds the optimal gear and engine state using dynamic programming. The control strategy is then applied to several test cases to evaluate its performance and to compare the fuel consumption of different types and sizes of platoons. Most notably, the test cases show that the fuel consumption can be reduced up to 10 % with a platoon of four hybrid electric vehicles compared to the single vehicle case. Finally, the results are discussed and possible future work is suggested.

Keywords: energy optimization, platooning, hybrid electric vehicle, model predictive control, dynamic programming, adaptive cruise controller, cooperative adaptive cruise controller.

Acknowledgements

We would like to thank our supervisors Nikolce Murgovski and Jonas Fredriksson from the department of Electrical Engineering at Chalmers University of Technology for their guidance and support throughout the project. We also would like to thank Martin Sanfridson at Volvo Group for making this project possible by providing us with model data and valuable inputs.

Mattias Hovgard and Oscar Jonsson
Gothenburg, June 2017

Contents

List of Figures	xi
List of Tables	xv
Mathematical Symbols	xvii
1 Introduction	1
1.1 Background	2
1.2 Aim	2
1.3 Contributions	3
1.4 Delimitations	3
1.5 Method	3
1.6 Thesis Outline	4
2 Physical Modelling	5
2.1 Single vehicle	5
2.1.1 Vehicle model	5
2.1.2 ICE model	7
2.1.3 EM model	9
2.1.4 Battery model	12
2.2 Multiple vehicles	12
2.2.1 Safety constraints	13
2.2.2 Aerodynamic drag reduction	13
3 Control Strategy	15
3.1 Overview	15
3.2 Hierarchical control scheme	17
3.3 Top optimization layer	18
3.3.1 Change of variables	18
3.3.2 Simplifications and approximations	19
3.3.3 Final SOCP formulation	22
3.4 Bottom optimization layer	23
3.4.1 Power split	24
3.4.2 Dynamic programming	26
3.4.3 Finding the fuel equivalent	26
3.5 Summary of control strategy	27

4	Results	29
4.1	Case studies with a single vehicle	29
4.1.1	Conventional vehicle with fixed velocity	30
4.1.2	Conventional vehicle with varying velocity	31
4.1.3	HEV with fixed velocity	32
4.1.4	HEV with varying velocity	33
4.2	Case studies with multiple vehicles	34
4.2.1	Benefit of platooning	36
4.2.2	Benefit with varying velocity	37
4.2.3	Benefit with HEV	38
4.3	Special investigations	39
4.3.1	Mixed platoon of conventional vehicles and HEVs	39
4.3.2	Velocity variation	40
4.3.3	Reduced air drag coefficient	41
4.3.4	Reduced mass	41
4.4	Computation time performance	42
5	Discussion	45
5.1	Validity of the models and results	45
5.2	Sustainability and ethical aspects	46
6	Conclusion	47
7	Future Work	49
	Bibliography	51
A	Model Parameters	I
B	Pre-filter to Obtain Feasible Reference Speed	III
C	Additional Details from Case-studies	V

List of Figures

2.1	Overview of the powertrain of an HEV, showing how the ICE, electric machine (EM), battery, gearbox and differential gear are connected. Note that the ICE is connected to the driving shaft, while the EM is connected to the countershaft via an additional gear. This means that the EM and ICE will have different gear ratios.	6
2.2	Fuel consumption of the ICE plotted as a function of torque for some different engine speeds. The circles represent measured data and the lines are the fitted function, which is quadratic in torque.	7
2.3	Torque limits of the ICE plotted as a function of engine speed. The dashed line represents the measured data and the solid lines are the fitted functions. The efficiency of the ICE is also shown.	8
2.4	Positive torque limits of the EM as a function of engine speed. The dashed lines are the measured data and the solid lines are the fitted functions. The efficiency of the electric machine is also shown.	9
2.5	Negative torque limits of the EM as a function of engine speed. The dashed lines are the measured data and the solid lines are the fitted functions. The dot-dashed line depicts the maximum charging power of the battery. The efficiency of the EM is also shown.	10
2.6	Power consumption of the electric machine as a function of torque for some different engine speeds. The circles represent measured data and the lines are the fitted function, which is quadratic in torque.	11
2.7	Several vehicles forming a platoon in a hilly terrain.	12
2.8	Total air drag reduction for each vehicle in a platoon of size 3. It is assumed that the bumper to bumper distance between each of the vehicles is the same. At short distances the reduction is greater for a vehicle that has one vehicle in front and one behind than for a vehicle that has two vehicles ahead. This can be seen in the figure where the lines for the middle and trail vehicle are crossing.	14
3.1	The road altitudes for the driving cycles mainly used when solving the optimization problem.	16
3.2	Illustration of the hierarchical control scheme which consists of two layers. The top layer finds the optimal speed and optimal battery costate. Using this information, the bottom layer finds the optimal gear and ICE state. Note that the bottom layer optimization can be done separately for each of the vehicles.	17
3.3	Flowchart of the complete algorithm including the two optimization layers.	28

4.1	The velocity trajectory for a conventional vehicle with fixed velocity as a function of traveled distance. The plot also shows the optimal gear choice.	30
4.2	The forces acting on a conventional vehicle with fixed velocity as function of traveled distance. The plot shows the optimal force from the ICE and the braking force.	30
4.3	The velocity trajectory for a conventional vehicle with varying velocity as a function of traveled distance. The plot also shows the optimal gear choice. . . .	31
4.4	The forces acting on a conventional vehicle with varying velocity as function of traveled distance. The plot shows the optimal force from the ICE and the braking force.	31
4.5	The velocity and SOC trajectories for an HEV with fixed velocity as a function of traveled distance. The plot also shows the optimal gear choice and ICE state.	32
4.6	The forces acting on an HEV with fixed velocity as function of traveled distance. The plot shows the optimal force from the ICE, EM and the braking force. The ICE state is also presented.	33
4.7	The velocity and SOC trajectories for an HEV with varying velocity as a function of traveled distance. The plot also shows the optimal gear choice and ICE state.	33
4.8	The forces acting on an HEV with varying velocity as function of traveled distance. The plot shows the optimal force from the ICE, EM and the braking force. The ICE state is also presented.	34
4.9	Inter-vehicle distance measured in time between the vehicles in a platoon consisting of four vehicles. The different lines represent the time distance between different vehicles, in this case 3 distances.	34
4.10	Velocity, gear and ICE status for all vehicles in a platoon of size four, plotted on top of each other.	35
4.11	Comparisons of the losses from air resistance and braking forces between an average platoon member (of a platoon with four vehicles) and a single vehicle, both for conventional vehicle and HEV.	36
4.12	The improvement in average fuel consumption per vehicle of platooning from size 2 to size 5 for different types of vehicles compared to the fuel consumption for a single vehicle for respective type.	37
4.13	The improvement in average fuel consumption per vehicle of allowing the velocity to vary within an interval compared of having a fixed velocity. Both conventional vehicles and HEVs in platoons up to size 5 are presented.	38
4.14	The improvement in average fuel consumption per vehicle when comparing conventional vehicles with HEVs of the same platoon size. Both vehicles with fixed and varying velocity in platoons up to size 5 are presented.	38
4.15	The improvement in average fuel consumption per vehicle for conventional vehicles and HEVs in a 4-vehicle platoon for different sizes of the allowed velocity interval Δ_v compared to having a fixed velocity for the platoon.	40
4.16	Average computation time on a standard PC (Intel Core i5-2450M 2.5 GHz and 4 GB RAM), for one iteration of each of the two optimization layers as a function of horizon length and platoon size. The computation time for the top layer seems to increase quadratic or exponential with both those things, while for the lower layer the increment is linear.	43

4.17	Total computation time of the control algorithm with a platoon of four vehicles as a function of horizon length. The computations are done on a standard PC (Intel Core i5-4200U 2.30 GHz and 8 GB RAM).	43
C.1	Comparison of the velocity profiles between a light (18.5 t) 4-vehicle platoon and a heavy (41.8 t) 4-vehicle platoon, for all the members of the platoon.	VI
C.2	Comparison of the velocity profiles between a 4-vehicle platoon with low air resistance ($c_d = 0.3$) and 4-vehicle platoon ($c_d = 0.6$), for all the members of the platoon.	VI

List of Tables

0.1	Table of the mathematical symbols for the variables.	xvii
4.1	Average fuel consumption per vehicle measured in 1/100 km for different types of vehicles and platoon sizes. The number of vehicles in the platoon is represented by N	35
4.2	Average fuel consumption per vehicle when there are 2 conventional vehicles and 2 HEVs in a platoon. The position of the conventional vehicles in the platoon is marked with \boxtimes , and the platoon is driving to the right.	39
4.3	Improvement in average fuel consumption per vehicle for different air drag coefficients. The comparisons are made between a single HEV vs a 4-vehicle platoon of HEVs and between a 4-vehicle platoon of conventional vehicles vs a platoon of HEVs with the same size.	41
4.4	Improvement in average fuel consumption per vehicle for different masses. The comparisons are made between a single HEV vs a 4-vehicle platoon of HEVs and between a 4-vehicle platoon of conventional vehicles vs a platoon of HEVs with the same size.	42
A.1	Values of the model parameters that are used in the case studies.	I
C.1	Improvement in fuel consumption (1/100 km) per vehicle for a platoon of 4 vehicles compared to a single vehicle for different allowed velocity intervals. Each vehicle type (CV and HEV) are compared to their own single vehicle type. . . .	V
C.2	Average fuel consumption per vehicle for a 4-vehicle platoon of conventional vehicles and HEVs and for a single HEV, for different values of the aerodynamic constant c_d	V
C.3	Average fuel consumption per vehicle for a 4-vehicle platoon of conventional vehicles and HEVs and for a single HEV, for different masses.	V

Mathematical Symbols

Table 0.1: Table of the mathematical symbols for the variables.

Variable	Unit	Description
s	m	Distance
t	s	Time
v	m/s	Velocity of vehicle
E_V	J	Kinetic energy of vehicle
T_E	N m	Torque from ICE
ω_E	rad/s	Speed of ICE
F_E	N	Force from ICE
P_E	W	Power from ICE
T_M	N m	Torque from EM
ω_M	rad/s	Speed of EM
F_M	N	Force from EM
P_M	W	Power from EM
F_{brk}	N	Force from mechanical brakes
P_{brk}	W	Power from mechanical brakes
F_B	N	Force from battery
P_B	W	Power from battery
E_B	J	Battery energy
λ_B	kg/J	Costate of battery energy
P_{Td}	W	Power losses from transitions and transmissions
γ	-	Gear
u_γ	-	Gear change command
χ	-	ICE state
u_χ	-	ICE state change command
α	rad	Road slope
μ	kg/s	Fuel consumption
d_{ji}	m	Inter-vehicle distance between vehicle i and j

1

Introduction

Reducing the energy consumption of moving vehicles is desirable for several reasons. One of them is to reduce the fuel costs, and low fuel consumption is an important selling point for vehicle manufactures. For example, a survey conducted by the American Transportation Research Institute [2] shows that US trucking companies 2014 on average spent 34% of their expenditures on fuel. In recent years, another driving factor have emerged, which is the desire to reduce the negative effects vehicle emissions have on human health and the environment. According to the European Environmental Agency, air pollution (which transportation is a major contributor to) in 2014 caused 40 000 deaths in the European Union alone [3]. On the subject of global warming, data from Eurostat shows that around 23% of the greenhouse emissions in the European Union 2014 came from transportation [4].

One way to reduce energy consumption is to utilize some form of Adaptive Cruise Controller (ACC) [5], and use information from the surrounding environment (e.g. topography of the road ahead) to optimize the speed, and thereby save fuel. For example, it is unnecessary to speed up just before a downhill and then have to use the mechanical brakes to not exceed the speed limits. If the vehicle instead is aware of the downhill ahead, it does not have to speed up, and less energy will be wasted due to mechanical braking. However, because of surrounding traffic and speed limits etc. some energy will inevitably be wasted using the mechanical brakes. This issue can to some extent be solved using a Hybrid Electric Vehicle (HEV), since an HEV can utilize its electric machine for braking. In other words, transferring the kinetic energy of the vehicle to electric energy, which can be stored in a battery and later be used, thus saving additional fuel. Furthermore, an HEV can turn off the engine during parts of the driving cycle, which also saves fuel.

A more advanced version of ACC is the Cooperative Adaptive Cruise Controller (CACC) [6]. A CACC communicates information between vehicles, making it possible to form tight vehicle formations, known as platooning. With this comes another possibility to save fuel, namely to reduce the air resistance the vehicles are exposed to during movement. This is a major contributing factor of fuel consumption for trucks, since there are limitations to how aerodynamically efficient they can be built. With the CACC, the vehicle distance can be kept very small (compared to the case with only manual control) and a significantly reduced air resistance for the members of the platoon can be achieved, even for the leading vehicle.

1.1 Background

There are many techniques to minimize the fuel consumption for conventional vehicles by using information of the road ahead. One such technique is presented by [7] which uses a Model Predictive Controller (MPC) [8] that is solved using Dynamic Programming (DP) [9]. However, due to the rapid increase in states when considering a platoon of vehicles, DP becomes impractical. Therefore, optimization of an entire platoon often involves dividing the optimization into multiple sub-problems. Some examples are three earlier master projects ([10], [11] and [12]) as well as an article [13] published in the subject. In these projects, MPCs are designed which optimizes the velocity and gear selection separately. The velocity is optimized by formulating the problem as a convex optimization problem which can be solved efficiently using commercial solvers. The gear selection is optimized using DP or simply by always choosing the highest possible gear. The conclusion is that up to 10 % can be saved when traveling in a platoon compared to alone. However, they only looked at conventional vehicles and recent development suggests that HEVs will play a major role in the transportation systems in the future, and more research are conducted in that area [14].

Energy optimization of HEVs is more complex than that of conventional vehicles. This is mainly because any optimization strategy must manage an additional energy storage, the electric battery. It also introduces extra states, the battery state of charge (SOC) and engine on/off state, as well as extra control signals for deciding electric machine power and turning the engine on or off. Energy optimization for a single HEV has previously been examined in [15] and [7]. The former uses MPC and formulates the velocity optimization as a Quadratic programming (QP) problem, and a separate DP-scheme to optimize the gear selection. The decision of when to turn on/off the engine is managed by filtering the result from the QP-problem and using a simple rule of thumb about how often the engine can be turned on. The results show that up to 5 % of fuel can be saved compared to a conventional vehicle. The authors in [7] introduces a method utilizing fuel equivalents which relates the use of electric energy to fuel consumption, to manage the battery energy. It seems reasonable to assume that when combining the use of HEVs with the possibility to drive in platoons and to adjust the velocity depending on the road ahead, a significant reduction of fuel consumption can be achieved.

1.2 Aim

The main aim of this project is to construct a control strategy for optimizing speed, battery SOC, travel time, gear and engine state for a number of HEVs, traveling in a platoon, on a road with a known topography. A secondary aim is to use the above-mentioned control strategy, with different road profiles as well as different combinations of vehicles with different properties and compare them to each other. This will give insight to what the optimal control strategy for different types of platoons are, as well the difference in fuel consumption. For example, how much fuel can be saved by using a platoon of HEVs, compared to a single HEV or platoon with conventional vehicles?

1.3 Contributions

This project uses a similar control strategy as [13]. The main contribution is to extend the control strategy to also include HEVs. This means that the mathematical descriptions of the electric machine and battery are included in the problem formulation. These descriptions are also simplified to fit the convex optimization formulation. The DP is modified to be able to handle the discrete decision of when to turn on/off the engine. This is made possible using fuel equivalents for the energy management of the battery. Additionally, some interesting test-cases are examined to compare the optimal control strategy of HEVs to conventional vehicles.

1.4 Delimitations

The control strategy is only designed to find the optimal solutions. If it is to be used in a real vehicle, some additional work must be done. First, the control strategy will probably have to be simplified, to make it more efficient to solve. A control layer will also have to be added, to compensate for the model mismatch between the ideal models used in the controller, and the actual dynamics of the vehicles. In case studies, only perfect driving conditions are assumed and no other vehicles are present. It is also assumed that the vehicles never have to slow down or stop for traffic lights for example. This project is limited to only consider optimization of the entire platoon as a whole. Another alternative would be to use a greedy approach, where each vehicle is optimized separately. Furthermore, the models that are used, such as the model of the vehicles and the air drag, are deterministic, and stochastic models are not in the scope of this project.

1.5 Method

Already existing control strategies and how to model hybrid vehicles are studied with the help from the literature and previous works in the area. A mathematical formulation of the control strategy is then created, which is simplified in several different ways in order to make it efficient to use. This includes dividing the optimization into two sub-problems and making these sub-problems convex. The simplified mathematical formulation is then implemented in MATLAB (version 2016b from The MathWorks Inc), and solved using an optimization software called CVX (version 2.1 from CVX Research, Inc.) [16]. Finally, different test cases are designed and carried out, to evaluate the performance of the control strategy.

1.6 Thesis Outline

The thesis starts with the modelling in Chapter 2, which contains all of the physical models used in this project. First for a single HEV, including the power equations regarding the movement of the vehicles and the power balance of the electrical components, as well as models of the vehicle components. Then the models are adapted to multiple HEVs and models for the air drag reduction are included. The control strategy is presented in Chapter 3, which starts with an overview of the optimization problem, which is then divided into two different optimization layers, a top layer and a bottom layer. The top optimization layer is described in Section 3.3, where it is first simplified using linearization and variable changes, before the final form is presented. The bottom optimization layer is presented in Section 3.4. A summary of the complete control algorithm is given in Section 3.5. In Chapter 4, some case studies and results are presented, which includes the sections: single vehicle, multiple vehicles, special investigations and performance. A discussion about the results and the project as a whole can be found in Chapter 5. Finally, a conclusion and suggestions for future work are presented in Chapter 6 and 7 respectively.

2

Physical Modelling

This chapter describes the physical model of an HEV as well as how multiple vehicles interact with each other. The models are mainly inspired from [13], and the model data are provided from Volvo Group. More details about the model parameters can be found in Table A.1 in Appendix A.

2.1 Single vehicle

In this section, models of the components in an HEV are presented, as well as the differential equations of the mechanical and electrical power balance.

2.1.1 Vehicle model

An overview of an HEV is presented in Figure 2.1. The vehicle is equipped with an Internal Combustion Engine (ICE), which either can be on or off, as well as an Electric Machine (EM). The EM is powered by a battery, which in turn can be charged by the EM by using it as a generator. Both the ICE and EM are connected to the same gearbox. However the ICE is connected to the driving shaft, while the EM is connected to the countershaft via an additional gear. This means that the EM and ICE will have different gear ratios. The HEV can be modeled as a lumped mass with two real valued dynamic states, the velocity v and the battery energy E_B . There are also two integer states γ , χ which represents the gear and ICE state (on/off) respectively. Therefore, the model is a hybrid system with mixed real- and integer valued states and control signals dependent on the time t .

The equation of motion of the vehicles has the form

$$m_e \dot{v}(t) = F_V(t) - F_{Vd}(v(t), \alpha(s(t))) - mg \sin(\alpha(s(t))) \quad (2.1)$$

where m is the mass, m_e is the equivalent mass which includes the actual vehicle mass and terms representing inertia of rotational parts. The force F_V is the total traction force delivered at the wheels, g is the gravitational acceleration, and α is the road gradient which is a function of the distance traveled $s(t)$. Lastly, F_{Vd} represent dissipative forces depending on the air- and

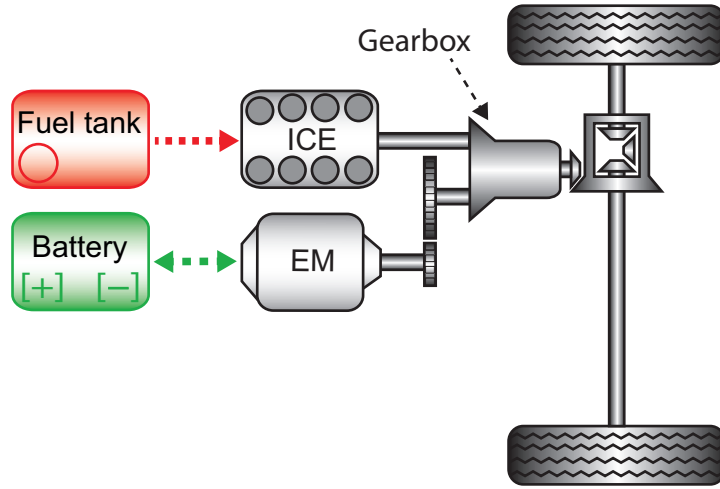


Figure 2.1: Overview of the powertrain of an HEV, showing how the ICE, electric machine (EM), battery, gearbox and differential gear are connected. Note that the ICE is connected to the driving shaft, while the EM is connected to the countershaft via an additional gear. This means that the EM and ICE will have different gear ratios.

rolling resistance, which are modeled as

$$F_{Vd}(v(t), \alpha(s(t))) = F_{\text{air}}(v(t)) + F_{\text{rol}}(\alpha(s(t))) = \frac{\rho_a A_f c_d}{2} v^2(t) + mgc_r \cos(\alpha(s(t))) \quad (2.2)$$

where ρ_a is the air density, A_f is the frontal area of the truck, c_d is the aerodynamic drag coefficient and c_r is the rolling resistance coefficient.

The mechanical power balance is expressed as

$$P_E(t) + P_M(t) - P_{\text{brk}}(t) = F_V(t)v(t) + P_{\text{Td}}(\gamma(t), \chi(t), P_E(t), P_M(t), u_\gamma(t), u_\chi(t)) \quad (2.3)$$

where P_E is the power from the ICE, P_M is the power from the EM, $P_{\text{brk}} \geq 0$ is the mechanical braking power and P_{Td} includes all power dissipation from transitions and state changes as well as losses in the transmissions.

The electrical power balance is expressed as

$$P_B(t) = P_M(t) + P_{\text{Md}}(v(t), P_M(t)) + P_{\text{Bd}}(P_B(t)) + P_A \quad (2.4)$$

where P_B is the battery power, P_{Md} and P_{Bd} are the dissipative power from the electric machine and the battery respectively. P_A is the power consumed by auxiliary devices and is simplified to have a constant value.

The gear and ICE state are defined in the domains Γ and X respectively, and can take the values

$$\gamma \in [1, \dots, \gamma_{\text{max}}], \quad \chi \in [0(\text{off}), 1(\text{on})]. \quad (2.5)$$

The states in the next time instance γ^+ , χ^+ is a function of the current state and the commands to switch gear, $u_\gamma \in U_\gamma = [-1, 0, 1]$ and change state of the ICE $u_\chi \in U_\chi = [-1, 0, 1]$,

$$\gamma^+ = \gamma + u_\gamma, \quad (2.6)$$

$$\chi^+ = \chi + u_\chi. \quad (2.7)$$

Each time the gear is changed or the ICE is turned on, some additional fuel is used, which is represented by W_γ and W_χ respectively.

2.1.2 ICE model

The fuel consumption of the ICE, denoted μ , depends both on the torque T_E and the engine speed ω_E of the ICE. It can be described by fitting a function to the measurements of the fuel rate over torque and engine speed and is formulated as

$$\mu(\omega_E(t), T_E(t)) = a_0 + a_1\omega_E(t) + a_2\omega_E^3(t) + a_3\omega_E^5(t) + a_4\omega_E(t)T_E(t) + a_5\omega_E(t)T_E^2(t). \quad (2.8)$$

The measurements and fitted model can be observed in Figure 2.2. It turns out that a good fit can be obtained by putting the coefficients a_1 and a_2 to zero, so that model is used from now on. The engine torque T_E and angular velocity ω_E can be related to the vehicle speed v and longitudinal force F_E delivered by the ICE as

$$\omega_E(t) = r_E(\gamma)v(t), \quad T_E(t) = \frac{F_E(t)}{\eta r_E(\gamma)} \quad (2.9)$$

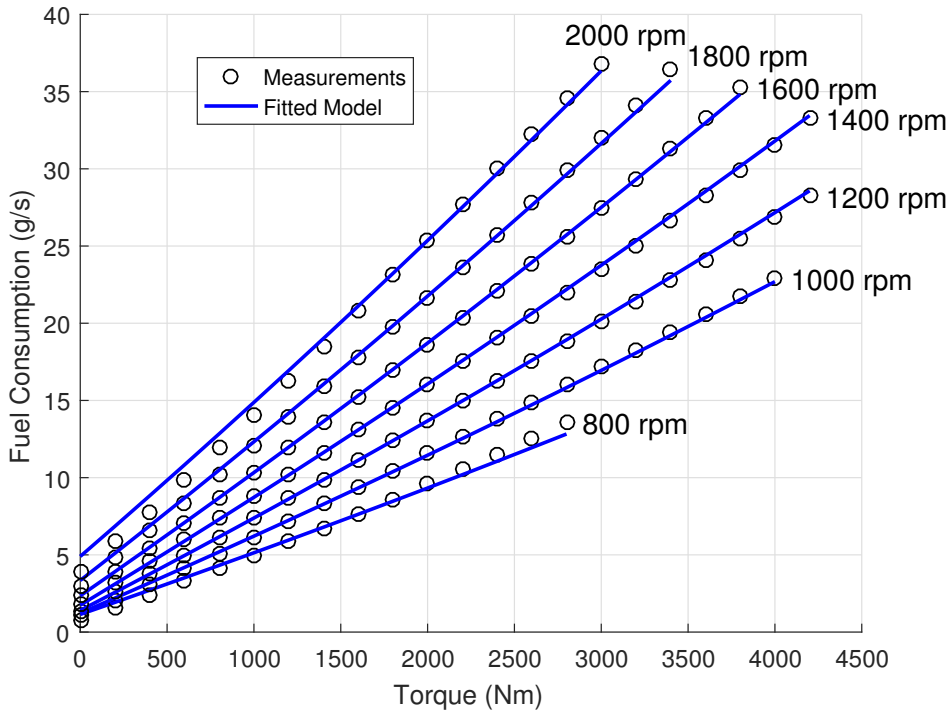


Figure 2.2: Fuel consumption of the ICE plotted as a function of torque for some different engine speeds. The circles represent measured data and the lines are the fitted function, which is quadratic in torque.

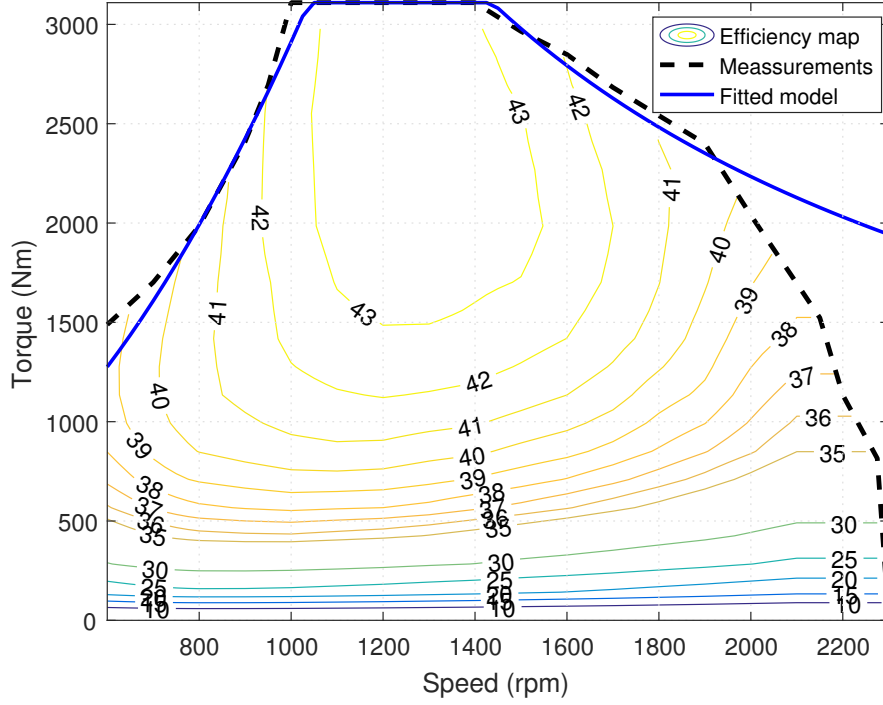


Figure 2.3: Torque limits of the ICE plotted as a function of engine speed. The dashed line represents the measured data and the solid lines are the fitted functions. The efficiency of the ICE is also shown.

where η is the efficiency from the engine to the wheels and represents losses in the transmission, and r_E is defined as

$$r_E(\gamma) = \frac{r_E^f(\gamma)}{R_w} \quad (2.10)$$

where $r_E^f(\gamma)$ is the total gear ratio of the gearbox to the ICE including the differential gear for gear γ , and R_w is the radius of the wheels. The maximum torque the engine can deliver as a function of engine speed is plotted in Figure 2.3. After converting to force and vehicle speed using equation (2.9), the longitudinal force limits can be formulated with three constraints. The first constraint is approximated by a quadratic function of the vehicle speed,

$$F_E(t) \leq \eta r_E(\gamma) (b_1 + b_2 r_E^2(\gamma) v^2(t)). \quad (2.11)$$

The second one depends on the peak engine torque b_0 ,

$$F_E(t) \leq \eta r_E(\gamma) b_0. \quad (2.12)$$

The third constraint depends on the rated engine power $P_{E\max}$,

$$F_E(t) \leq \frac{\eta P_{E\max}}{v(t)}. \quad (2.13)$$

Finally, the delivered force can not be negative,

$$F_E(t) \geq 0. \quad (2.14)$$

Note that with this formulation it is assumed that the ICE cannot be used to brake, that is included in the mechanical braking force instead. To express these constraints in terms of power, the constraints (2.13)-(2.14) are multiplied with the velocity v , which in a more compact form gives

$$\begin{aligned} P_E(t) &\leq \eta P_{E\max}, \\ P_E(t) &\in \eta r_E(\gamma) v(t) \left[0, \min \left\{ b_0, b_1 + b_2 r_E^2(\gamma) v^2(t) \right\} \chi(t) \right]. \end{aligned} \quad (2.15)$$

Note that the last expression includes χ to ensure that the ICE cannot deliver any force when it is off.

2.1.3 EM model

For the EM the total ratio r_M between the engine and the wheels are calculated as

$$r_M(\gamma) = \frac{r_M^f(\gamma)}{R_w}, \quad (2.16)$$

where $r_M^f(\gamma)$ is the total ratio of the gearbox and the differential gear to for gear γ . The relationship between the angular velocity ω_M and the vehicle speed v is similar as for the ICE,

$$\omega_M(t) = r_M(\gamma) v(t). \quad (2.17)$$

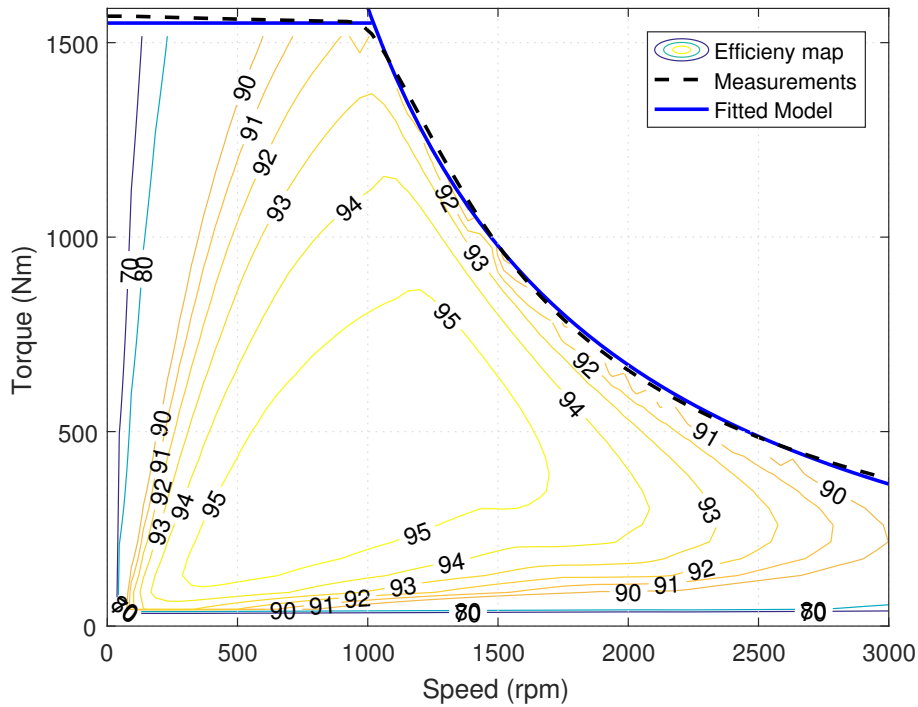


Figure 2.4: Positive torque limits of the EM as a function of engine speed. The dashed lines are the measured data and the solid lines are the fitted functions. The efficiency of the electric machine is also shown.

The relationship between the torque T_M from the EM to the force F_M at the wheels are also similar as for the ICE. However, how the efficiency of the transmission is included depends on if the EM is used for propulsion of the vehicle or as a generator,

$$T_M(t) = \begin{cases} \frac{F_M(t)}{\eta r_M(\gamma)} & \text{if } F_M(t) \geq 0 \\ \frac{\eta F_M(t)}{r_M(\gamma)} & \text{if } F_M(t) < 0 \end{cases} \iff T_M(t) = \frac{1}{r_M(\gamma)} \max \left\{ \frac{F_M(t)}{\eta}, \eta F_M(t) \right\}. \quad (2.18)$$

The maximum torque delivered by the EM is modeled with the functions

$$T_{M\max}(t) = \min \left\{ c_{12}, \frac{c_{21}}{\omega_M(t)} + c_{22} \right\} \quad (2.19)$$

where c_{12} , c_{21} and c_{22} , are constants to fit measurements of the maximum torque data. An illustration of the measurement data, fitted data as well as the efficiency of the EM can be seen in Figure 2.4. Similar constraints can be found for the negative torque

$$T_{M\min}(t) = \max \left\{ b_{12}, \frac{b_{21}}{\omega_M(t)} + b_{22}, \frac{P_{B\max}}{\omega_M(t)} \right\}. \quad (2.20)$$

Note however that an additional constraint has been added, which depends on the maximum charging power of the battery ($P_{B\max}$), and has been included here for convenience. The measurements, the efficiency for the EM as well as the modeled constraints are plotted in

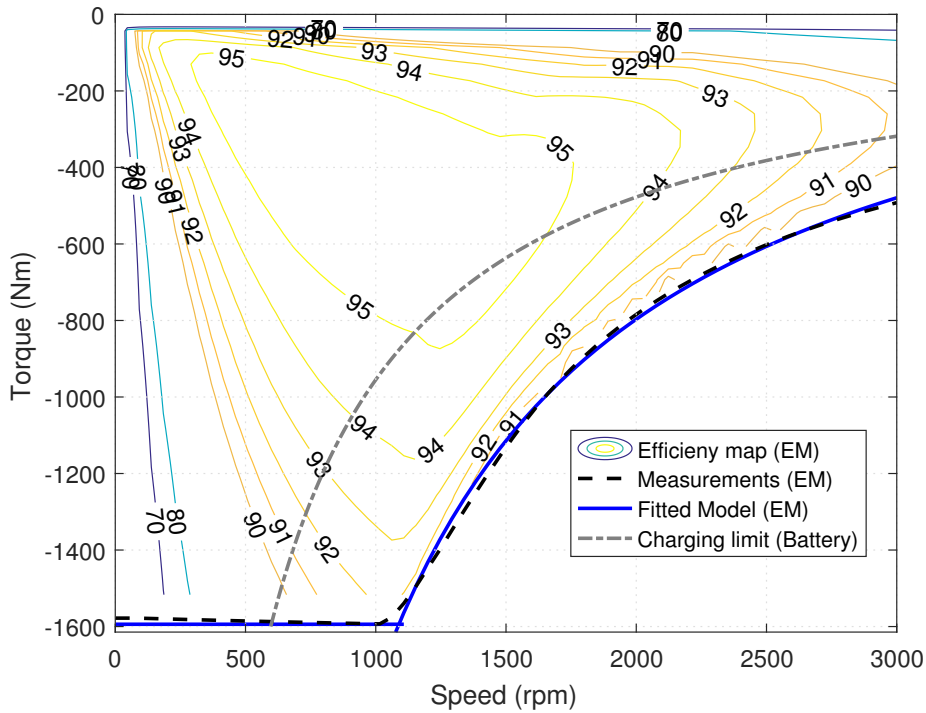


Figure 2.5: Negative torque limits of the EM as a function of engine speed. The dashed lines are the measured data and the solid lines are the fitted functions. The dot-dashed line depicts the maximum charging power of the battery. The efficiency of the EM is also shown.

Figure 2.5. The maximum/minimum wheel force delivered by the EM becomes

$$\begin{aligned} F_{M\max}(t) &= \eta r_M(\gamma) \min \left\{ c_{12}, \frac{c_{21}}{r_M(\gamma)v(t)} + c_{22} \right\}, \\ F_{M\min}(t) &= \frac{r_M(\gamma)}{\eta} \max \left\{ b_{12}, \frac{b_{21}}{r_M(\gamma)v(t)} + b_{22}, \frac{P_{B\max}}{r_M(\gamma)v(t)} \right\}. \end{aligned} \quad (2.21)$$

The maximum/minimum power of the EM is obtained by multiplying (2.21) with the velocity v , which yields

$$\begin{aligned} P_{M\max}(t) &= \eta r_M(\gamma)v(t) \min \left\{ c_{12}, \frac{c_{21}}{r_M(\gamma)v(t)} + c_{22} \right\}, \\ P_{M\min}(t) &= \frac{r_M(\gamma)v(t)}{\eta} \max \left\{ b_{12}, \frac{b_{21}}{r_M(\gamma)v(t)} + b_{22}, \frac{P_{B\max}}{r_M(\gamma)v(t)} \right\}. \end{aligned} \quad (2.22)$$

The power losses from the EM is modeled as

$$P_{Md}(t) = h_1\omega_M(t) + h_2\omega_M^3(t) + h_3\omega_M^5(t) + h_4\omega_M(t)T_M(t) + h_5\omega_M(t)T_M^2(t), \quad (2.23)$$

where the constants h_j , $j = 1, \dots, 5$, are obtained from fitting a function to measured data. Similar to the model of the fuel consumption some constants are put to zero, in this case h_1 and h_3 . The power losses in terms of force and velocity then becomes

$$P_{Md}(t) = h_2r_M^3(\gamma)v^3(t) + h_4v(t) \max \left\{ \frac{F_M(t)}{\eta}, \eta F_M(t) \right\} + \frac{h_5v(t)}{r_M(\gamma)} \max \left\{ \frac{F_M(t)}{\eta}, \eta F_M(t) \right\}^2. \quad (2.24)$$

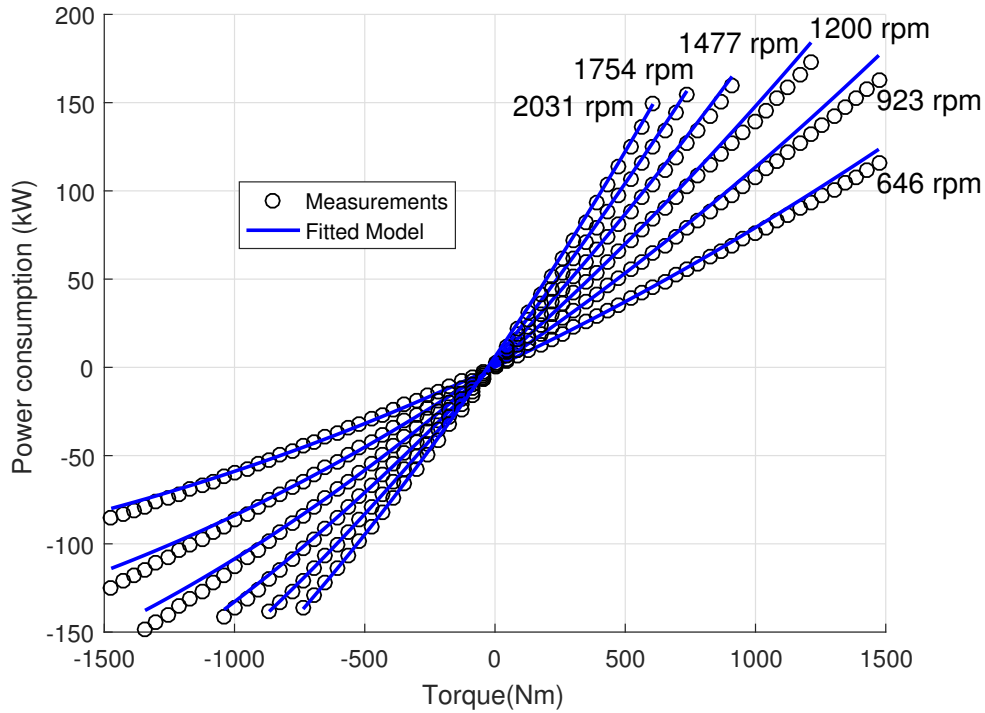


Figure 2.6: Power consumption of the electric machine as a function of torque for some different engine speeds. The circles represent measured data and the lines are the fitted function, which is quadratic in torque.

The total power consumed by the EM ($P_M + P_{Md}$) is plotted in Figure 2.6.

2.1.4 Battery model

The energy of the battery is a state which is governed by the following equation

$$\dot{E}_B(t) = -P_B(t). \quad (2.25)$$

It is assumed that there is no limit on how much power the battery can deliver and a charging limit has already been included in the EM model. The only constraint left regarding the battery is the minimum and maximum usable energy,

$$E_B(t) \in [\text{SOC}_{\min}, \text{SOC}_{\max}] E_{B\max}, \quad (2.26)$$

where $E_{B\max}$ is the maximum energy capacity of the battery and SOC_{\min} , SOC_{\max} limits the lower and upper bounds of the state of charge (SOC) which is defined as

$$\text{SOC} = \frac{E_B(t)}{E_{B\max}}. \quad (2.27)$$

The power loss of the battery is modeled using a constant open voltage (V_{oc}) in series with a constant resistance (R),

$$P_{Bd}(t) = \frac{R}{V_{oc}^2} P_B^2(t). \quad (2.28)$$

2.2 Multiple vehicles

With multiple vehicles two additional factors must be taken into consideration, safety constraints and air drag reduction. Several vehicles in a platoon are illustrated in Figure 2.7. The equations and models presented above are applied to all the vehicles, and in order to distinguish the mathematical expressions between different vehicles, the subscript i is added to the variables denoting that they belong to the vehicle $i = 1, \dots, N$, where N is the number of vehicles in the platoon.

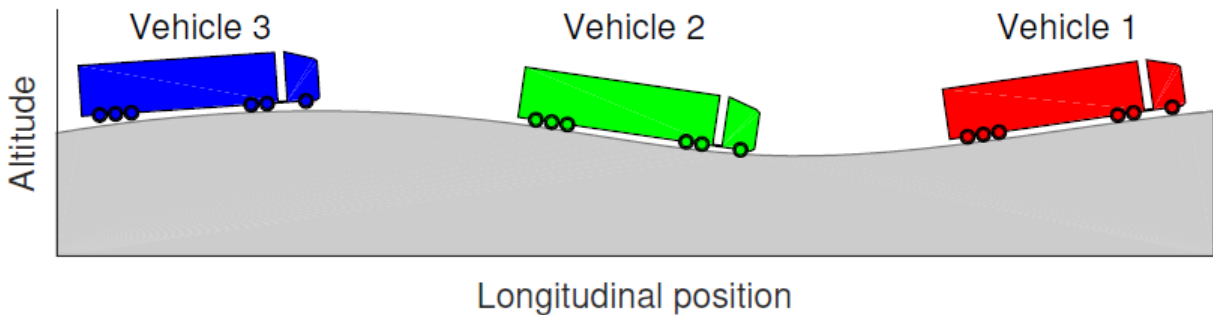


Figure 2.7: Several vehicles forming a platoon in a hilly terrain.

2.2.1 Safety constraints

To prevent that the vehicles drive too close to each other, there are safety constraints included in the formulation. They are expressed as

$$t_i \geq t_{i-1} + t_{hi}, \quad (2.29)$$

which states that the vehicles must at minimum have a time headway of t_{hi} . The time headway is defined as the time it takes for vehicle i to reach the current position of vehicle $i - 1$. This can also be represented as a minimum distance headway constraint as

$$d_{ji}(t) \geq d_{hi}, \quad (2.30)$$

where d_{hi} is the minimum distance between the vehicles. The variable d_{ji} is the distance between vehicle i and j and is defined as

$$d_{ji}(t) = |s_j(t) - s_i(t)| - L_{ji}, \quad (2.31)$$

where s_i and s_j are the longitudinal position of the vehicles, and L_{ji} is a parameter depending on the length of the vehicles. The position s_i can be obtained from

$$\dot{s}_i(t) = v_i(t), \quad (2.32)$$

together with the initial value $s_i(t_0) = s_{0i}$.

2.2.2 Aerodynamic drag reduction

While driving in a platoon, the vehicles experience aerodynamic drag reduction caused by the other nearby vehicles around. The effect depends on several factors, for example vehicle geometry, speed, and inter-vehicle distance. The air drag reduction model that is implemented is a function depending of the inter-vehicle distance and consists of three contributions from the nearby surrounding vehicles; the pull from the two closest vehicles ahead and the push from the vehicle directly behind. The aerodynamic drag is modelled as

$$F_{airi}(v_i(t), d_{ji}(t)) = F_{airi}^o(v_i(t)) \left(1 - \sum_j f_d(d_{ji}(t)) \right), \quad (2.33)$$

where F_{airi}^o is the air resistance if no other vehicles are present nearby. The sum represents the total air drag reduction from the surrounding vehicles $j = \{i + 1, i - 1, i - 2\} \cap \{1, \dots, N\}$ on the vehicle i . $i + 1$ is the vehicle behind, $i - 1$ is the first vehicle in front and $i - 2$ and is the second vehicle in front. The air drag reduction function f_d is modeled as a sum of two exponential functions

$$f_d(d_{ji}(t)) = a_{1ji} \exp(-b_{1ji}d_{ji}(t)) + a_{2ji} \exp(-b_{2ji}d_{ji}(t)) \quad (2.34)$$

where the constants $a_{1ji}, a_{2ji}, b_{1ji}, b_{2ji}$ are obtained by fitting measurement data. A comparison of the total air drag reduction between the measurements and fitted model can be seen in Figure 2.8.

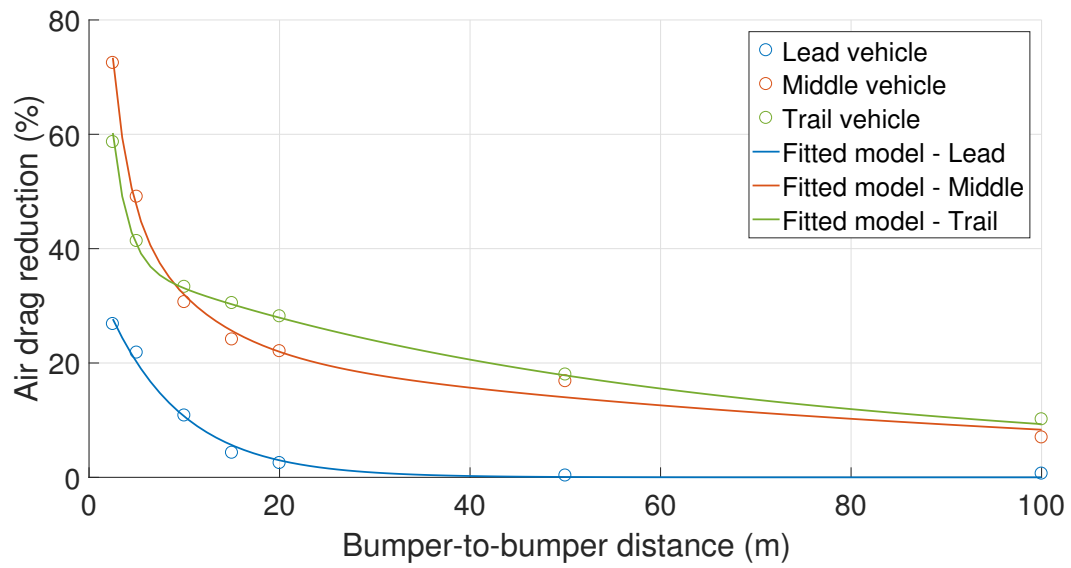


Figure 2.8: Total air drag reduction for each vehicle in a platoon of size 3. It is assumed that the bumper to bumper distance between each of the vehicles is the same. At short distances the reduction is greater for a vehicle that has one vehicle in front and one behind than for a vehicle that has two vehicles ahead. This can be seen in the figure where the lines for the middle and trail vehicle are crossing.

3

Control Strategy

This chapter includes an in-depth description of the control strategy used to minimize the fuel consumption of a vehicle-platoon. It also presents the simplifications made to the problem to reduce complexity and make it more efficient to solve.

3.1 Overview

The controller is a predictive CACC which aims at finding the optimal trajectories for the states: velocity v^* , battery energy E_B^* , traveled distance s^* , gear γ^* and ICE state χ^* , which minimizes the total energy consumed by all the member vehicles of a platoon over the horizon $t \in [t_0, t_f]$. Note that the horizon in this case consists of the whole driving cycle and that the optimization is only run once. The control signals are the real valued powers P_E, P_M and P_{brk} , and the integer variables u_γ and u_χ .

It is assumed that the vehicles are given a constant cruising speed \bar{v} . However, they may not be able to keep the cruising speed in steep uphill. Therefore, the reference speed \hat{v} is lowered in those parts of the driving cycle where the vehicles cannot drive with the cruising speed. More details of how to obtain the reference velocity can be found in Appendix B. The vehicles are allowed to vary their speed $\pm\Delta_v$ from the reference speed. With a given driving cycle the total horizon length in distance $s_f - s_0$ can be obtained. Since the reference velocity is known as a function of time, the total travel time for the driving cycle with this velocity can be calculated. This time is denoted T_{max} which constrains the final time as $t_f \leq t_0 + T_{max}$. This means that even if the velocity is allowed to vary from the reference, the vehicles still have to complete the driving cycle within the same time frame as if they were driving with the reference speed. It is also assumed that the battery have the same charge, or higher, at the end of the horizon as it started with. Therefore the only relevant aspect to take into account in the cost function is the total fuel consumed by the ICE.

Two different driving cycles are mainly used for the vehicles to travel on and they are presented in Figure 3.1. One is a short driving cycle that is 20 km long. It is used with the purpose for illustrations, and the sample distance for the cycle is 80 m. The other cycle is the Borås-Landvetter-Borås driving cycle (BLB), and represents the real road between Borås and Landvetter. It is 86.9 km long and will be used when comparing data between different

3. Control Strategy

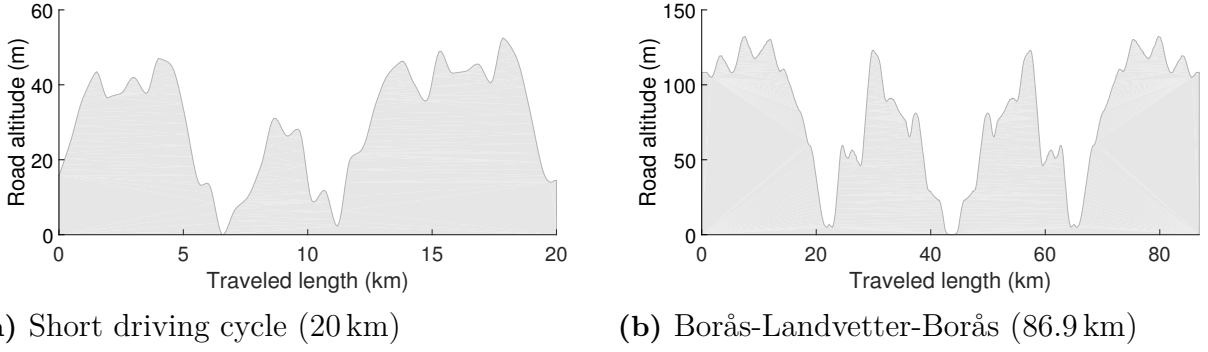


Figure 3.1: The road altitudes for the driving cycles mainly used when solving the optimization problem.

configurations. The sample distance for this cycle is 100 m.

The optimization problem for a platoon of vehicles ($i = 1, \dots, N$) is formulated as

$$\text{minimize } J = \sum_{i=1}^N \left(\int_{t_0}^{t_f} (\mu_i(\cdot) + W_{\gamma_i}(\cdot) + W_{\chi_i}(\cdot) + W_{c_i}(\cdot)) dt \right) \quad (3.1a)$$

subject to $\forall i = 1, \dots, N$

$$P_{Ei}(t) + P_{Mi}(t) - P_{brki}(t) = F_{Vi}(t)v_i(t) + P_{Tdi}(\cdot) \quad (3.1b)$$

$$P_{Bi}(t) = P_{Mi}(t) + P_{Mdi}(v_i(t), P_{Mi}(t)) + P_{Bdi}(P_{Bi}(t)) + P_{Ai} \quad (3.1c)$$

$$m_{ei}\dot{v}_i(t) = F_{Vi}(t) - F_{airi}(v_i(t), d_{ji}(t)) - m_i g(\sin(\alpha(s(t))) + c_r \cos(\alpha(s(t)))) \quad \forall j \in \{i+1, i-1, i-2\} \cap \{1, \dots, N\} \quad (3.1d)$$

$$\dot{E}_{Bi}(t) = -P_{Bi}(t) \quad (3.1e)$$

$$\dot{s}_i(t) = v_i(t) \quad (3.1f)$$

$$v_i(t_0) = v_{0i} \quad (3.1g)$$

$$v_i(t) \in [v_{\min i}(t), v_{\max i}(t)] \quad (3.1h)$$

$$s_i(t_0) = s_{0i}, \quad s_i(t_f) = s_{fi} \quad (3.1i)$$

$$t \in [t_0, t_f] \quad (3.1j)$$

$$t_f - t_0 \leq T_{\max} \quad (3.1k)$$

$$P_{Ei}(t) \leq \eta P_{E\max i}, \quad (3.1l)$$

$$P_{Ei}(t) \in \eta r_E(\gamma_i(t))v_i(t) \left[0, \min \{b_0, b_1 + b_2 r_E^2(\gamma_i(t))v_i^2(t)\} \chi_i(t) \right] \quad (3.1m)$$

$$P_{Mi}(t) \in [P_{M\min i}(v_i(t), \gamma_i(t)), P_{M\max i}(v_i(t), \gamma_i(t))] \quad (3.1n)$$

$$P_{brki}(t) \geq 0 \quad (3.1o)$$

$$E_{Bi}(t_0) = E_{B0i}, \quad E_{Bi}(t_f) \geq E_{Bfi} \quad (3.1p)$$

$$E_{Bi}(t) \in [\text{SOC}_{\min i}, \text{SOC}_{\max i}] E_{B\max i} \quad (3.1q)$$

$$\gamma_i^+(t) = \gamma_i(t) + u_{\gamma_i}(t), \quad \gamma_i(t) \in \Gamma, \quad u_{\gamma_i}(t) \in U_{\gamma} \quad (3.1r)$$

$$\chi_i^+(t) = \chi_i(t) + u_{\chi_i}(t), \quad \chi_i(t) \in X, \quad u_{\chi_i}(t) \in U_{\chi} \quad (3.1s)$$

$$d_{ji}(t) \geq d_{hi} \quad i = 2, \dots, N, \quad j = i - 1 \quad (3.1t)$$

The term W_c is a comfort penalty, which purpose is to penalize non-smooth behavior. Note that the losses from the transmission (except the once caused by the transitions) have been included by using the constant efficiency (η), so the term P_{Td} now only includes losses from transitions and state changes. This optimization problem contains both real valued and integer optimization variables and states. These types of problems are hard and computationally demanding to solve. Therefore, a hierarchical control scheme will be presented, which divides the optimization problem into layers.

3.2 Hierarchical control scheme

An overview of the hierarchical control scheme can be seen in Figure 3.2. It consists of two layers, which both tries to minimize the cost function (3.1a), but with regards to different variables.

- The **top layer** uses given gear (γ) and ICE state (χ) trajectories to find the optimal values of the states: velocity (v), distance (s) and battery energy (E_B) for all the member vehicles of the platoon. The control signals are the powers from the ICE (P_E), EM (P_M) and braking (P_{brk}). The optimization problem is solved using convex optimization. The top layer sends the optimal velocity as well as the optimal costate (λ_B) corresponding to

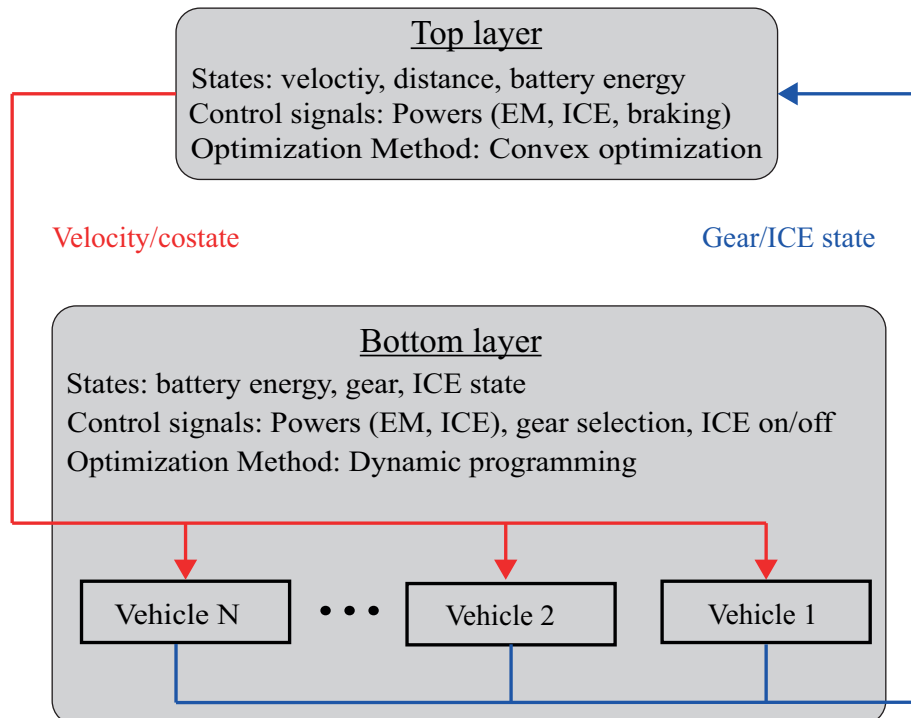


Figure 3.2: Illustration of the hierarchical control scheme which consists of two layers. The top layer finds the optimal speed and optimal battery costate. Using this information, the bottom layer finds the optimal gear and ICE state. Note that the bottom layer optimization can be done separately for each of the vehicles.

the optimal battery energy, to the bottom layer. The costate commonly referred to as fuel equivalent and is discussed further in Section 3.4.

- The **bottom layer** uses dynamic programming to find the optimal gear (γ) and ICE state (χ). The control signals are the power from the ICE and EM as well as the gear select and ICE on/off commands. The bottom layer can be solved completely separately for each of the vehicles.

These two layers are solved iteratively until the solution converge (more on this in Section 3.5).

3.3 Top optimization layer

The top optimization layer is similar to the original optimization formulation (3.1), but the main difference is that the discrete decision variables have been removed. However, additional simplifications must be made in order to make the problem more efficient to solve. Most importantly the problem needs to be made convex [17]. If an optimization problem is convex it can be written on the form

$$\text{minimize } f(x) \quad (3.2)$$

$$\text{subject to } g(x) \leq 0, \quad i = 1, \dots, m \quad (3.3)$$

$$h(x) = 0, \quad i = 1, \dots, p \quad (3.4)$$

Where the functions f, g_1, \dots, g_m are convex, and h_1, \dots, h_p are affine. For example, 2.11 is a constraint that cannot be written on this form. Note that the max-function, that is used in some of the constraints, are convex as long as the inputs are convex. Similarly, the min-function is concave as long as its inputs are concave.

3.3.1 Change of variables

The first step is to reformulate the optimization problem from time domain to space domain, thus making the traveled distance (s) an independent variable instead of time (t). This makes time a state with the dynamics

$$t'(s) = \frac{dt}{ds} = \frac{1}{v(s)}. \quad (3.5)$$

Another advantage of sampling in distance rather than in time is that the data of the road topography is given in space coordinates, and it would be more complicated and more inaccurate to convert the data as a function of time. When working in space domain it is more convenient to work with forces instead of powers. Therefore, the following variable changes are introduced

$$F_E(s) = \frac{P_E(s)}{v(s)}, \quad F_M(s) = \frac{P_M(s)}{v(s)}, \quad F_B(s) = \frac{P_B(s)}{v(s)}, \quad F_{\text{brk}}(s) = \frac{P_{\text{brk}}(s)}{v(s)}. \quad (3.6)$$

The fuel consumption is also modified as

$$\tilde{\mu}(\cdot) = \frac{\mu(\cdot)}{v(s)}. \quad (3.7)$$

where $\tilde{\mu}(\cdot)$ denotes the fuel consumption per distance traveled. The next step is to express the optimization problem in terms of kinetic energy instead of velocity,

$$E_V(s) = \frac{m_e v^2(s)}{2}. \quad (3.8)$$

This is a common strategy and has been used in previous works. It makes some constraints linear, for example (2.11). Finally, with these variable changes, the state equations for the vehicle and the battery energy are also modified and become

$$\begin{aligned} m_e \dot{v}(t) &\implies E'_V(s), \\ \dot{E}_B(t) = -P_B(t) &\implies E'_B(s) = -F_B(s). \end{aligned} \quad (3.9)$$

3.3.2 Simplifications and approximations

Due to the change of variables, expressions which are proportional to $1/v(s)$ will in turn be proportional to $1/\sqrt{E_V(s)}$. To make those expressions convex, the function

$$\frac{1}{v(s)} = f_t(E_V(s)) = \sqrt{\frac{m_e}{2E_V(s)}}, \quad (3.10)$$

is linearized around the reference kinetic energy $\hat{E}_V(s)$, which is simply the kinetic energy of the vehicle when driving with the reference speed. The linearization yields

$$f_t^{\text{lin}}(E_V(s)) = \sqrt{\frac{m_e}{2\hat{E}_V(s)}} + \left. \frac{\partial f_t}{\partial E_V} \right|_{\hat{E}_V} \Delta E_V(s), \quad (3.11)$$

where $\Delta E_V(s) = E_V(s) - \hat{E}_V(s)$. This linearization is for example applied on the term consisting of the auxiliary power, thus $P_A/v(s) \approx P_A f_t^{\text{lin}}(E_V(s))$. The subscript t in f_t denotes that $f_t = t'(s)$.

3.3.2.1 ICE model

Since the gear trajectory is already set when solving problem (3.1), it is possible that the ICE is unable to deliver enough force to keep a velocity within the limits. This is very likely if the gear is chosen poorly and may cause infeasibility. The force delivered from the ICE F_E is therefore divided into two forces

$$F_E(s) = F_{E1}(s) + F_{E2}(s), \quad (3.12)$$

where $F_{E1}(s)$ is the force delivered from the current gear and $F_{E2}(s)$ is a force that possibly could be delivered for any other choice of gear. $F_{E2}(s)$ is an abstract force and will only be used if $F_{E1}(s)$ fails to deliver a force satisfying (2.11). The constraints for the force limits of the ICE will in the new variables have the form

$$F_{E1}(s) + F_{E2}(s) \leq \eta P_{E\max} \sqrt{\frac{m_e}{2E_V(s)}} \quad (3.13)$$

which is linearized using (3.11) and yielding

$$F_{E1}(s) + F_{E2}(s) \leq \eta P_{E\max} f_t^{\text{lin}}(E_V(s)). \quad (3.14)$$

The constraint for F_{E1} is now expressed as

$$F_{E1}(s) \in \eta r_E(\gamma) \left[0, \min \left\{ b_0, b_1 + \frac{2b_2 r_E^2(\gamma)}{m_e} E_V(s) \right\} \chi(s) \right]. \quad (3.15)$$

3.3.2.2 Electric machine model

The constraints of the wheel force from EM will in the new variables have the form

$$\begin{aligned} F_{M\max}(E_V(s)) &= \eta r_M(\gamma) \min \left\{ c_{12}, \frac{c_{21}}{r_M(\gamma)} \sqrt{\frac{m_e}{2E_V(s)}} + c_{22} \right\}, \\ F_{M\min}(E_V(s)) &= \frac{r_M(\gamma)}{\eta} \max \left\{ b_{12}, \frac{b_{21}}{r_M(\gamma)} \sqrt{\frac{m_e}{2E_V(s)}} + b_{22}, \frac{P_{B\max}}{r_M(\gamma)} \sqrt{\frac{m_e}{2E_V(s)}} \right\}. \end{aligned} \quad (3.16)$$

Since this does not define a convex set, the constraints are linearized using (3.11). This gives the constraints

$$\begin{aligned} F_{M\max}(E_V(s)) &= \eta r_M(\gamma) \min \left\{ c_{12}, \frac{c_{21}}{r_M(\gamma)} f_t^{\text{lin}}(E_V(s)) + c_{22} \right\}, \\ F_{M\min}(E_V(s)) &= \frac{r_M(\gamma)}{\eta} \max \left\{ b_{12}, \frac{b_{21}}{r_M(\gamma)} f_t^{\text{lin}}(E_V(s)) + b_{22}, \frac{P_{B\max}}{r_M(\gamma)} f_t^{\text{lin}}(E_V(s)) \right\}. \end{aligned} \quad (3.17)$$

The force losses from the electric machine will in the new variables become

$$F_{Md}(s) = \frac{2h_2 r_M^3(\gamma)}{m_e} E_V(s) + h_4 \max \left\{ \frac{F_M(s)}{\eta}, \eta F_M(s) \right\} + \frac{h_5}{r_M(\gamma)} \max \left\{ \frac{F_M(t)}{\eta}, \eta F_M(t) \right\}^2, \quad (3.18)$$

which is an equality that is linear in $E_V(s)$ but quadratic in $F_M(s)$, which is a problem. As mentioned earlier equality constraints must be affine in the variables, which this expression is not. To solve this issue, (3.18) is relaxed to become an inequality constraint instead (replace $=$ with \geq). This makes the convex expression at the right side allowed. This modification does not affect the solution. At the optimum, equality will hold anyway because it will always be optimal for the losses to be as small as possible.

3.3.2.3 Battery model

The battery force dissipation in the new variables becomes

$$F_{\text{Bd}}(s) = \frac{R}{V_{\text{oc}}^2} \sqrt{\frac{2E_{\text{V}}(s)}{m_e}} F_{\text{B}}^2(s) \approx \frac{R}{V_{\text{oc}}^2} \sqrt{\frac{2\hat{E}_{\text{V}}(s)}{m_e}} F_{\text{B}}^2(s), \quad (3.19)$$

where the kinetic energy is replaced with its reference to avoid multiplying different optimization variables, which would have made the problem non-convex. Note that the losses is quadratic in $F_{\text{B}}(s)$.

3.3.2.4 Aerodynamic drag model and safety constraints

The aerodynamic drag reduction will in the new variables have the form

$$F_{\text{air}i}(E_{\text{V}i}(s), d_{ji}(s)) = F_{\text{air}i}^o(E_{\text{V}i}(s)) \left(1 - \sum_j f_d(d_{ji}(s)) \right). \quad (3.20)$$

with $j = \{i + 1, i - 1, i - 2\} \cap \{1, \dots, N\}$. The function $f_d(d_{ji}(s))$ is both nonlinear and non-convex and thereby a linearization is made around $\hat{d}_{ji}(s)$ which denotes the inter-vehicle distance that is computed from the reference velocity of vehicle i and j . After linearizing around both $\hat{E}_{\text{V}i}(s)$ and $\hat{d}_{ji}(s)$ the air drag reduction model becomes

$$F_{\text{air}i}^{\text{lin}}(E_{\text{V}i}(s), d_{ji}(s)) = c_a E_{\text{V}i}(s) \left(1 - \sum_j f_d(\hat{d}_{ji}(s)) \right) - c_a \hat{E}_{\text{V}i}(s) \sum_j (d_{ji}(s) - \hat{d}_{ji}(s)) \left. \frac{\partial f_d}{\partial d_{ji}} \right|_{\hat{d}_{ji}}, \quad (3.21)$$

with $c_a = \frac{\rho_a A_f c_d}{m_{ei}}$ and $\hat{E}_{\text{V}i}(s)$ is the reference kinetic energy for vehicle i . The inter-vehicle distance $d_{ji}(s)$ is now expressed as

$$d_{ji}(s) = |x_j(s) - x_i(s)| - L_{ji}, \quad (3.22)$$

where $x_i(s)$ and $x_j(s)$ are the longitudinal position of the vehicles as before but is now a function of the space coordinate s . By putting $x_1(s) = s$, the positions for the vehicles behind will be obtained from

$$x'_i(s) = \frac{v_i(s)}{v_1(s)}, \quad (3.23)$$

which is both a nonlinear and non-convex function. Equation (3.23) is instead approximated by linearizing around $1/\hat{v}_i(s)$ and $1/\hat{v}_1(s)$ which results in

$$x'_i(s) \approx \frac{\hat{v}_i(s)}{\hat{v}_1(s)} (1 + \hat{v}_1(s)t'_1(s) - \hat{v}_i(s)t'_i(s)). \quad (3.24)$$

With the assumption that the velocities $\hat{v}_i(s)$ do not vary too much from the cruising velocity \bar{v} , the simplification that $\hat{v}_i(s)$ can be replaced with $\hat{v}_i(s) \approx \bar{v}$ in (3.24) is made. By integrating (3.24) on both sides and insert in (3.22) results in

$$d_{ji}(s) \approx |x_{0i} - x_{0j} + \bar{v}((t_j(s) - t_{0j}) - (t_i(s) - t_{0i}))| - L_{ji}. \quad (3.25)$$

The first vehicle has the properties $x_1(0) = 0$ and $t_1(0) = 0$. Since the vehicles are not controlled until they reach position zero, the vehicles are considered to drive with the cruising velocity \bar{v} until then, which gives $x_{0i} = -\bar{v}t_{0i}$ and simplifies (3.25) to

$$d_{ji}(s) \approx \bar{v}|t_j(s) - t_i(s)| - L_{ji}. \quad (3.26)$$

Finally the safety constraint will become

$$t_i(s) \geq t_{i-1}(s) + t_{hi}, \quad (3.27)$$

where $t_i(s)$ is the time for vehicle i when it reaches the position s .

3.3.3 Final SOCP formulation

The complete simplified top layer optimization problem results in a convex Second Order Cone Problem (SOCP), which is formulated as

$$\text{minimize } \tilde{J} = \sum_{i=1}^N \left(\int_0^{s_f} (\tilde{\mu}_i(\cdot) + W_{\gamma_i}(\cdot) + W_{\chi_i}(\cdot) + W_{c_i}(\cdot) + q(E_{V_i}(s))) ds \right) \quad (3.28a)$$

subject to $\forall i = 1, \dots, N$

$$t'_i(s) = f_{ti}^{\text{lin}}(E_{V_i}(s)) \quad (3.28b)$$

$$E'_{V_i}(s) = F_{E1i}(s) + F_{E2i}(s) + F_{M_i}(s) - F_{brki}(s) + F_{airi}^{\text{lin}}(E_{V_i}(s), d_{ji}) + \\ - m_i g(\sin(\alpha(s)) + c_r \cos(\alpha(s))) \quad \forall j \in \{i+1, i-1, i-2\} \cap \{1, \dots, N\} \quad (3.28c)$$

$$E'_{B_i}(s) = -F_{B_i}(s) \quad (3.28d)$$

$$F_{B_i}(s) \geq \max \left\{ \frac{F_{M_i}(s)}{\eta}, \eta F_{M_i}(s) \right\} + F_{Mdi}(s) + F_{Bdi}(s) + P_{Ai} f_{ti}^{\text{lin}}(E_{V_i}(s)) \quad (3.28e)$$

$$t_i(s_f) \leq t_{fi} \quad (3.28f)$$

$$t_i(0) = t_{0i}, \quad E_{V_i}(0) = \frac{m_{ei} v_{0i}^2}{2} \quad (3.28g)$$

$$E_{V_i}(s) \in \frac{m_e}{2} [v_{\text{mini}}^2(s), v_{\text{maxi}}^2(s)] \quad (3.28h)$$

$$F_{E1i}(s) + F_{E2i}(s) \leq \eta P_{E\text{maxi}} f_{ti}^{\text{lin}}(E_{V_i}(s)) \quad (3.28i)$$

$$F_{E1i}(s) \in \eta r_E(\gamma) \left[0, \min \left\{ b_0, b_1 + \frac{2b_2 r_E^2(\gamma)}{m_{ei}} E_{V_i}(s) \right\} \chi(s) \right] \quad (3.28j)$$

$$F_{brki}(s) \geq 0, \quad F_{E2i} \geq 0 \quad (3.28k)$$

$$F_{M_i}(s) \in [F_{M\text{mini}}(E_{V_i}(s)), F_{M\text{maxi}}(E_{V_i}(s))] \quad (3.28l)$$

$$E_{B_i}(0) = E_{B0i}, \quad E_{B_i}(s_f) \geq E_{Bfi} \quad (3.28m)$$

$$E_{B_i}(s) \in [\text{SOC}_{\text{mini}}, \text{SOC}_{\text{maxi}}] E_{B\text{maxi}} \quad (3.28n)$$

$$t_i(s) \geq t_{i-1}(s) + t_{hi} \quad i = 2, \dots, N \quad (3.28o)$$

$$\gamma_i^+(s) = \gamma_i(s) + u_{\gamma_i}(s), \quad \gamma_i(s) \in \Gamma, \quad u_{\gamma_i}(s) \in U_\gamma \quad (3.28p)$$

$$\chi_i^+(s) = \chi_i(s) + u_{\chi_i}(s), \quad \chi_i(s) \in X, \quad u_{\chi_i}(s) \in U_\chi \quad (3.28q)$$

For each vehicle there are three states, t , E_V , and E_B , and four control signals, F_{E1} , F_{E2} , F_M , and F_{brk} . The term $q(\cdot)$ in the cost function represents a penalty term that depends of the linearization error of the kinetic energy. If this error is zero, then $q = 0$. The constraint (3.28e) is a relaxed version of (3.1c), which allows electric energy to be wasted. Wasting electric energy will only be optimal when no more energy can be put in the battery, (hitting the upper limit of (3.28n)), and the braking force comes into use.

The optimization problem is now convex and there exist efficient methods to solve such problems, for example the interior point method [18]. In this project, it is solved using a commercial solver named MOSEK (version 7.1.0.12 from Mosek ApS) [19].

3.4 Bottom optimization layer

The bottom layer receives the optimal speed and costate/fuel equivalent from the top layer and based on that the total demanded force F_V is found using (2.1). Even if F_V is known, how it is divided between F_M and F_E is not known and has to be calculated. This will be referred to as the power split. With the optimal power split, the optimal trajectories for gear can be calculated, and is returned to the top layer. Note that the results from the power split never is used outside of the bottom layer. The bottom layer solves the following optimization problem

$$\text{minimize } J = \int_0^{t_f} (\mu(F_E, \gamma, \chi) + W_\gamma(\gamma) + W_\chi(\chi)) dt \quad (3.29a)$$

$$\text{subject to} \quad (3.29b)$$

$$\dot{E}_B(F_M, \gamma, \chi) = -P_B(F_M, \gamma) \quad (3.29c)$$

$$F_V(t) = F_E(t) + F_M(t) \quad (3.29d)$$

$$P_B(F_M, \gamma, \chi) = \max \left\{ \frac{F_M(t)}{\eta}, \eta F_M(t) \right\} v(t) + P_{Md}(\gamma, F_M) + P_{Bd}(P_B) \quad (3.29e)$$

$$F_E(t) \leq \frac{\eta r_E(\gamma) P_{E\max}}{\omega(\gamma, \chi, t)} \quad (3.29f)$$

$$F_E(t) \in \eta r_E(\gamma) \left[0, \min \{ b_0, b_1 + b_2 \omega_E^2 \} \chi(t) \right] \quad (3.29g)$$

$$F_M(t) \leq \eta r_M(\gamma) \min \left\{ c_{12}, \frac{c_{21}}{\omega_M(\gamma, \chi, t)} + c_{22} \right\} \quad (3.29h)$$

$$F_M(t) \geq \frac{r_M(\gamma)}{\eta} \max \left\{ b_{12}, \frac{b_{21}}{\omega_M(\gamma, \chi, t)} + b_{22}, \frac{P_{B\max}}{\omega_M(\gamma, \chi, t)} \right\} \quad (3.29i)$$

$$E_{Bi}(t_0) = E_{B0i}, \quad E_{Bi}(t_f) \geq E_{Bfi} \quad (3.29j)$$

$$E_{Bi}(t) \in [\text{SOC}_{\min i}, \text{SOC}_{\max i}] E_{B\max i} \quad (3.29k)$$

$$\gamma^+(t) = \gamma(t) + u_\gamma(t), \quad \gamma(t) \in \Gamma, \quad u_\gamma(t) \in U_\gamma \quad (3.29l)$$

$$\chi^+(t) = \chi(t) + u_\chi(t), \quad \chi(t) \in X, \quad u_\chi(t) \in U_\chi \quad (3.29m)$$

This problem is similar to the original optimization problem (3.1), but here the constraints are expressed in terms of forces instead of powers. Also, since v^* is known, some constraints

have been removed. Note for example that the state equations for the time and velocity are no longer present and since this optimization can be done completely separate for each of the vehicles, the subscript i has been omitted. Problem (3.29) is solved using basic knowledge in optimal control theory [20]. The first step is to form the Hamiltonian.

$$\mathcal{H}(F_E, P_B, \gamma, \chi) = \mu(\gamma, \chi, F_E) + W_\gamma(\gamma) + W_\chi(\chi) - \lambda_B(t)P_B(\chi, \gamma, F_M), \quad (3.30)$$

where λ_B is the costate/fuel equivalent corresponding to (3.29d), and it is obtained from the top layer. Before presenting the solution, an important property for λ_B can be found by examining the necessary condition of optimality, namely

$$\left(\frac{\partial \mathcal{H}}{\partial E_B}\right)^* - \frac{d}{dt} \left(\frac{\partial \mathcal{H}}{\partial \dot{E}_B}\right)^* = 0 \implies \dot{\lambda}_B(t) = 0. \quad (3.31)$$

In other words, since neither μ , W_γ or W_χ is a function of E_B , λ_B is constant over time as long as E_B does not hit any constraint. In practice, it is likely that E_B does hit a constraint, which means that λ_B will be piecewise constant. However, in this project a large enough battery is used so that is never the case. Another property of λ_B is that it is negative. This can be concluded from the Hamiltonian, knowing that the cost should increase if the electric machine is used.

3.4.1 Power split

To solve (3.29) with regards to the power split, the Hamiltonian needs to be rewritten in terms of F_M (for the moment assuming that γ and χ are given). Starting with P_B

$$P_B = P_M + P_{Md}(F_M) + P_{Bd}(P_B) = \frac{\omega_M}{r_M} F_M + h_2 \omega_M^3 + \frac{h_4 \omega_M}{r_M} F_M + \frac{h_5 \omega_M}{r_M^2} F_M^2 + \frac{R}{V_{oc}^2} P_B^2. \quad (3.32)$$

This a polynomial of degree 2 in P_B and is solved using the quadratic formula, which gives the following expression

$$P_B(F_M) = \frac{V_{oc}^2}{2R} - \sqrt{\frac{V_{oc}^4}{4R^2} - \frac{h_2 \omega_M^3 V_{oc}^2}{R} - \frac{(h_4 + 1) \omega_M V_{oc}^2}{R r_M} F_M - \frac{h_5 \omega_M V_{oc}^2}{R r_M^2} F_M^2}. \quad (3.33)$$

The fuel consumption μ can be expressed in terms of F_M by simply substituting $F_E = F_V - F_M$. This gives the following expression for the Hamiltonian

$$\begin{aligned} \mathcal{H}(F_M) = & +a_0 + a_3 \omega_E^5 + \frac{a_4 \omega_E}{r_E} (F_V - F_M) + \frac{a_5 \omega_E}{r_E^2} (F_V - F_M)^2 - \lambda_B \frac{V_{oc}^2}{2R} + \\ & + \lambda_B \sqrt{\frac{V_{oc}^4}{4R^2} - \frac{h_2 \omega_M^3 V_{oc}^2}{R} - \frac{(h_4 + 1) \omega_M V_{oc}^2}{R r_M} F_M - \frac{h_5 \omega_M V_{oc}^2}{R r_M^2} F_M^2} + W_\gamma + W_\chi \end{aligned} \quad (3.34)$$

To simplify further calculations, the following constants are introduced

$$k_0 = a_0 + a_3 \omega_E^5 + \frac{a_4 \omega_E}{r_E} F_V + \frac{a_5 \omega_E}{r_E} F_V^2 - \lambda_B \frac{V_{oc}^2}{2R}, \quad (3.35)$$

$$k_1 = -\frac{a_4\omega_E}{r_E} - \frac{2a_5\omega_E}{r_E}F_V, \quad (3.36)$$

$$k_2 = \frac{a_5\omega_E}{r_E}, \quad (3.37)$$

$$k_3 = \frac{V_{oc}^4}{4R^2} - \frac{h_2\omega_M^3V_{oc}}{R}, \quad (3.38)$$

$$k_4 = -\frac{(h_4 + 1)\omega_M V_{oc}^2}{Rr_M}, \quad (3.39)$$

$$k_5 = -\frac{h_5\omega_M V_{oc}^2}{Rr_M^2}, \quad (3.40)$$

which simplifies (3.34) to

$$\mathcal{H}(F_M) = k_0 + k_1F_M + k_2F_M^2 + \lambda_B\sqrt{k_3 + k_4F_M + k_5F_M^2} + W_\gamma + W_\chi. \quad (3.41)$$

This function can be shown to always be convex. First of all, the terms that are constant or affine in F_M are all convex. The term $k_2F_M^2$ is also convex because k_2 is positive. Since λ_B is negative, the square root must be concave. It can be proven that a function $g(f(x))$ is concave, as long as $g(\cdot)$ is concave and nondecreasing, and $f(x)$ is concave. These conditions hold in this case since the square root function indeed is concave and nondecreasing, and k_5 is negative. Because (3.41) is convex, its minimum can be found by differentiating it with respect to F_M ,

$$\frac{\partial\mathcal{H}(F_M)}{\partial F_M} = k_1 + 2k_2F_M + \lambda_B\frac{k_4 + k_5F_M}{2\sqrt{k_3 + k_4F_M + k_5F_M^2}} = 0. \quad (3.42)$$

By rearranging and taking the square of the terms, (3.42) becomes

$$\lambda_B^2(k_4 + k_5F_M)^2 = 4(k_1 + 2k_2F_M)^2(k_3 + k_4F_M + k_5F_M^2). \quad (3.43)$$

Expanding the expression above gives a fourth order equation in F_M , which can be solved using the quartic formula [21]. The details will not be presented here but the solution will be referred to as F_M^a . This analytical solution does not take the constraints of the forces from the ICE and EM into consideration. If the analytical solution in fact does break any of the constraints, the solution will be on one of the constraints instead. Furthermore, if the ICE is off then $F_M = F_V$. To conclude how the optimal value of the Hamiltonian is found, the following formula is applied,

$$\mathcal{H}(F_M)^* = \begin{cases} \mathcal{H}(F_V) & , \chi = 0 \\ \mathcal{H}(F_M^a) & , F_{E\max} - F_V \leq F_M^a \leq F_{M\max} \\ \mathcal{H}(F_{M\max}) & , F_M^a \geq F_{M\max} \\ \mathcal{H}(F_{E\max} - F_V) & , F_M^a \leq F_{E\max} - F_V \end{cases} \quad (3.44)$$

Now, the optimal cost at each time and for a given gear and ICE state can be found. However, which combination of gear and engine states to use over the horizon is still left to decide. This will be solved using dynamic programming.

3.4.2 Dynamic programming

The state variables are the different gears and ICE state. The different combinations of the two state variables together creates the state $\xi = [\gamma, \chi]^T$. The DP starts at sample $k = K - 1$, where K is the number of samples. It then runs backwards in time and at each time instance and for each state, calculates the least possible cost to reach a feasible state at time K . This cost will be referred to as $J(\xi(k), k)$ and using Bellman's principle of optimality, it can be calculated as

$$J(\xi(k), k) = \min_{\xi(k+1) \in \Xi_{\text{feas}}} \{C(\xi(k), \xi(k+1), k) + J(\xi(k+1), k+1)\}, \quad (3.45)$$

where C is the cost of being at state ξ at time k , and is the optimal value of the Hamiltonian from (3.44). $\Xi_{\text{feas}} = [\Gamma_{\text{feas}}, X_{\text{feas}}]^T$ is the set of all the states at time $k + 1$ from where it is possible to reach state ξ at time k , and it is defined by

$$\Gamma_{\text{feas}} = \Gamma \cap (\gamma(k) + U_\gamma) \quad X_{\text{feas}} = X \cap (\chi(k) + U_\chi). \quad (3.46)$$

The penalty terms W_γ, W_χ (in the Hamiltonian) consists of a weight w_γ, w_χ and a variable y_γ, y_χ , which decides when the penalties should be added. The value of w_γ is tuned such that the gear is not changed too often. For example, if the gear is shifted up at one time instance and then shifted down again directly afterwards, that is probably not a desired behavior, and it is removed by increasing the value of w_γ . The value of w_χ is tuned such that when the engine has been turned on, it must run for at least 20s. The cost w_χ is added when the gear at time k is not the same as the gear at time $k + 1$. The cost w_χ is added if the engine is on at time $k + 1$ but not at time k . This can be expressed as

$$y_\gamma(\gamma(k), \gamma(k+1)) = \begin{cases} 1 & , \gamma(k) \neq \gamma(k+1) \\ 0 & , \text{otherwise} \end{cases} \quad (3.47)$$

$$y_\chi(\chi(k), \chi(k+1)) = \begin{cases} 1 & , \chi(k) = 0 \text{ and } \chi(k+1) = 1 \\ 0 & , \text{otherwise} \end{cases} \quad (3.48)$$

When the DP algorithm has reached time $k = 1$, it runs forward in time choosing the path with the least possible cost that reaches the final time $k = K$. This is calculated as

$$\xi^*(k+1) = \arg \min_{\xi(k+1) \in \Xi_{\text{feas}}} \{C(\xi^*(k), \xi(k+1), k) + J(\xi(k+1))\}, \quad (3.49)$$

where $\xi^*(k)$ is the optimal state at time k .

3.4.3 Finding the fuel equivalent

This bottom optimization problem (3.29) has similar properties to the top one (3.28), but there are some major differences, due to model mismatches between the two problems. Especially for long horizons it becomes apparent that the λ_B from the top layer is not the optimal one to be used in the bottom layer. It will provide a first good guess, but it will have to be improved

iteratively by running the DP algorithm multiple times. While running the DP algorithm E_B is calculated according to (3.29d). At the end of the horizon the error of E_B is calculated

$$E_B^{\text{error}} = E_B(0) - E_B(N) \quad (3.50)$$

For simplicity, it is assumed here that $E_B(0) = 0$, which simplifies (3.50) to $E_B^{\text{error}} = E_B(N)$. Knowing that the optimal λ_B must ensure that $E_B(N) \approx 0$, λ_B is adjusted accordingly after each iteration. For example, if $E_B(N) < 0$, λ_B must be bigger in order to penalize the use of the electric machine more. If $E_B(N)$ switches sign between two iterations, the optimal solutions have been passed, and the size of the adjustment can be decreased in order to improve the solution. The iterations continues until $E_B(N)$ are acceptably small. The whole procedure can be described using the following pseudo code:

1. run DP-algorithm, calculate $E_B^{[l]}(N)$.
2. If $E_B^{[l]}(N) \geq \text{threshold}$, go to 3. else end loop.
3. $\lambda_B^{[l+1]} = \lambda_B^{[l]} - \text{sign}(E_B(N)) \cdot \Delta$.
4. If $\text{sign}(E_B^{[l]}(N)) = -\text{sign}(E_B^{[l-1]}(N))$ go to 5, else go to 6.
5. $\Delta := \frac{\Delta}{2}$.
6. $l := l + 1$, go to 1.

3.5 Summary of control strategy

The complete optimization problem, including (3.28) and (3.29) is solved repeatedly until the solutions have converged within a certain tolerance level, or a maximum number of iterations have been reached. The algorithm is illustrated in Figure 3.3 and can be summarized as

1. Given a preferred cruise velocity, feasible reference speed trajectories $\hat{v}_i(s)$ are obtained for all vehicles in the platoon.
2. Gear trajectory, ICE state trajectory, and kinetic energy $\hat{E}_{V_i}(s)$ used for linearization are obtained. In the first iteration gear is guessed, e.g. highest gear all the time, the ICE is always on, and $\hat{E}_{V_i}(s)$ are calculated from the reference speed $\hat{v}_i(s)$. In the following iterations $\hat{E}_{V_i}(s)$ are obtained from the following equation,

$$\hat{E}_{V_i}^{(n+1)}(s) = \hat{E}_{V_i}^{(n)}(s) + \beta(E_{V_i}^{*(n)}(s) - \hat{E}_{V_i}^{(n)}(s)), \quad (3.51)$$

where (n) and $(n + 1)$ represent two following iterations and $\beta \in (0, 1]$ is the step size that affects the converging rate of the algorithm.

3. The top layer optimization problem (3.28) is solved and sends the optimal speed trajectory and costate/fuel equivalent to the bottom layer.

3. Control Strategy

4. The bottom layer optimization problem (3.29) is solved using the solution from step 3 to obtain the optimal gear and ICE state trajectories. This step may be iterated a number of times if needed to find a suitable costate/fuel equivalent.
5. For next update, go to step 2.

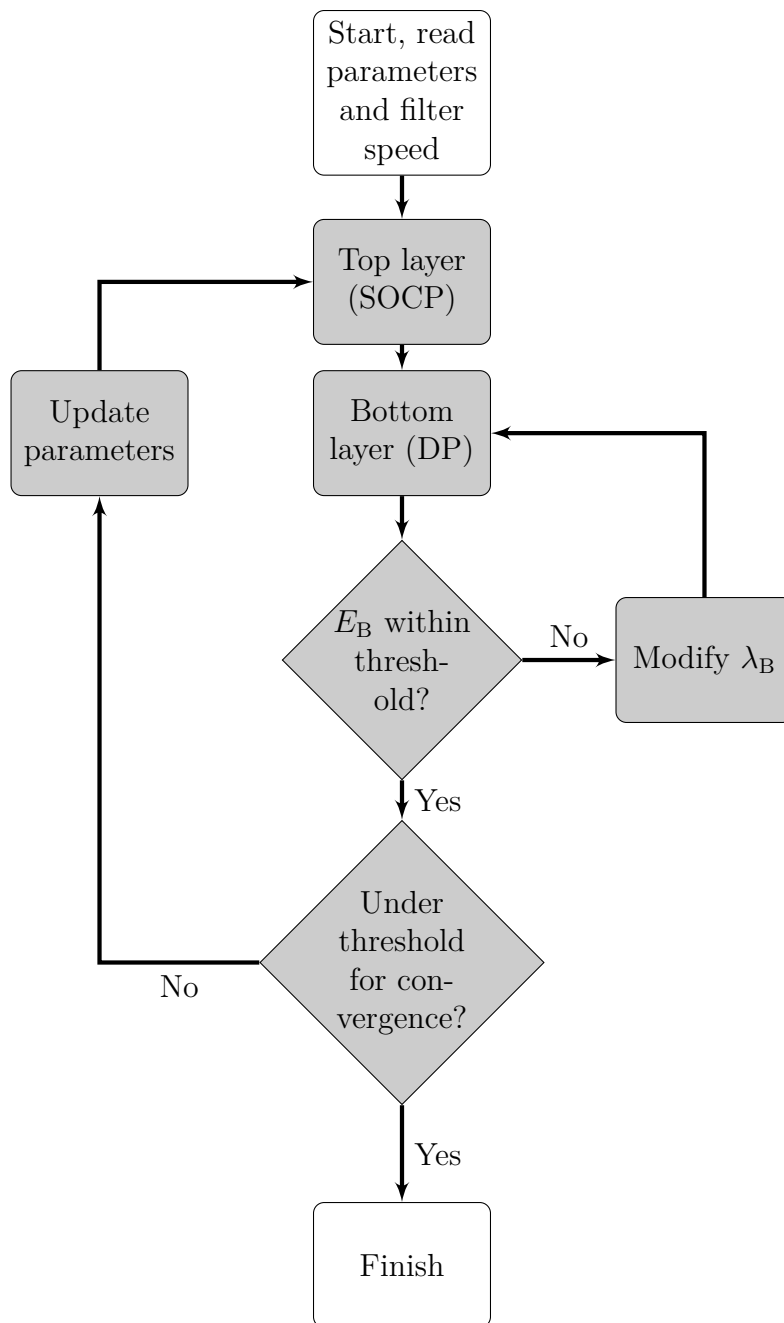


Figure 3.3: Flowchart of the complete algorithm including the two optimization layers.

4

Results

This chapter presents the results from some different case studies and comparisons between them. In the first part of the chapter only the case with a single vehicle is considered to show the basic functionality of the algorithm. The case with multiple vehicles is considered further down in the report, where the focus is mainly on the differences in fuel consumption between platoons of different types and sizes.

The following vehicle settings are chosen for the main case studies:

- Conventional vehicle with fixed velocity.
- Conventional vehicle with varying velocity.
- HEV with fixed velocity.
- HEV with varying velocity.

The settings with fixed velocity and conventional vehicle (sometimes referred to as CV) are only used to show what improvements that can be made by allowing the velocity to vary and using an HEV. The vehicles with varying velocity are allowed to vary ± 10 km/h from its reference and the mass of the vehicles are set to 41.8 t.

4.1 Case studies with a single vehicle

By investigate how a single vehicle behaves, some differences between the various vehicle settings can be seen. This is also a suitable approach to showcase the solutions given by the optimization algorithm. The small driving cycle of 20 km is used. The results that are presented contains the trajectories of the velocity, gear selection and ICE state, in addition to the forces acting on the system which are the control signals. First the case with a conventional vehicle is presented followed by the case with a hybrid vehicle.

4.1.1 Conventional vehicle with fixed velocity

The velocity trajectory along with the gear trajectory are shown in Figure 4.1 for a single conventional vehicle with fixed velocity. The road altitude is shown in the background. Note that in some uphill the velocity is forced to decrease in order to make the solution feasible. It is also shown that the vehicle is using a lower gear in the uphill and a higher gear in the downhill.

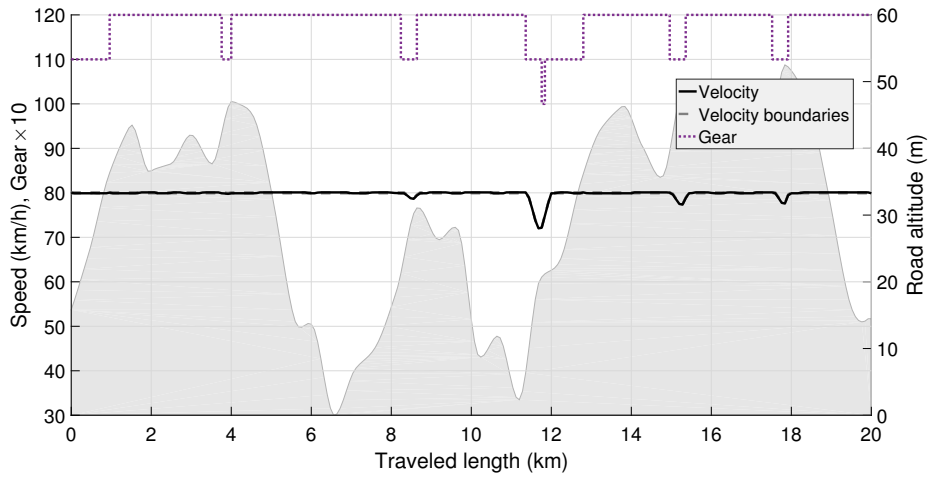


Figure 4.1: The velocity trajectory for a conventional vehicle with fixed velocity as a function of traveled distance. The plot also shows the optimal gear choice.

The forces acting on the vehicle can be seen in Figure 4.2, where the force from the ICE along with its limit as well as the braking force are shown. As expected the utilization of the ICE increases in the uphill and decreases in the downhill, were instead braking occurs to keep the fixed velocity.

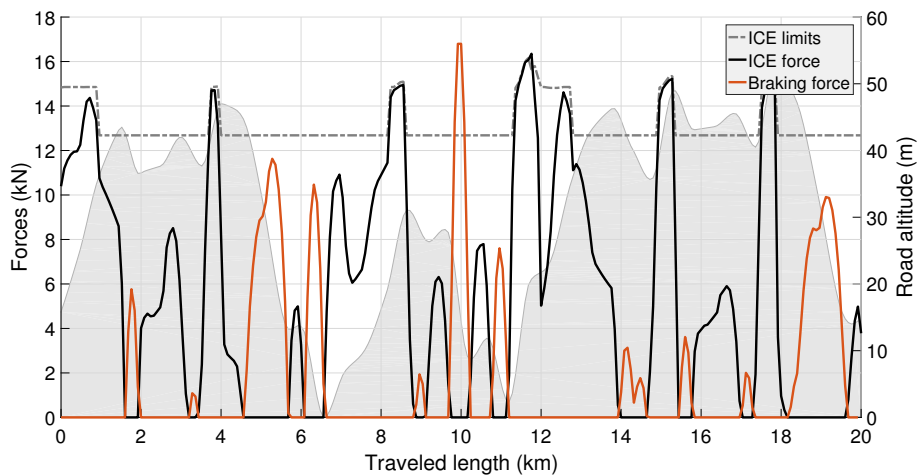


Figure 4.2: The forces acting on a conventional vehicle with fixed velocity as function of traveled distance. The plot shows the optimal force from the ICE and the braking force.

4.1.2 Conventional vehicle with varying velocity

The velocity trajectory along with the gear trajectory are shown in Figure 4.3 for a single conventional vehicle with varying velocity. The limits of the velocity are also shown. Note that the same gear is used during the whole driving cycle. The velocity profile shows that the velocity is at its lower limit just before a major downhill. It is increasing while the vehicle is driving down the hill and hit its upper limit at the end of the hill. This is because the solver is aware of the approaching downhill and by lowering its velocity, it can store the energy gained by the downhill as kinetic energy and avoids braking.

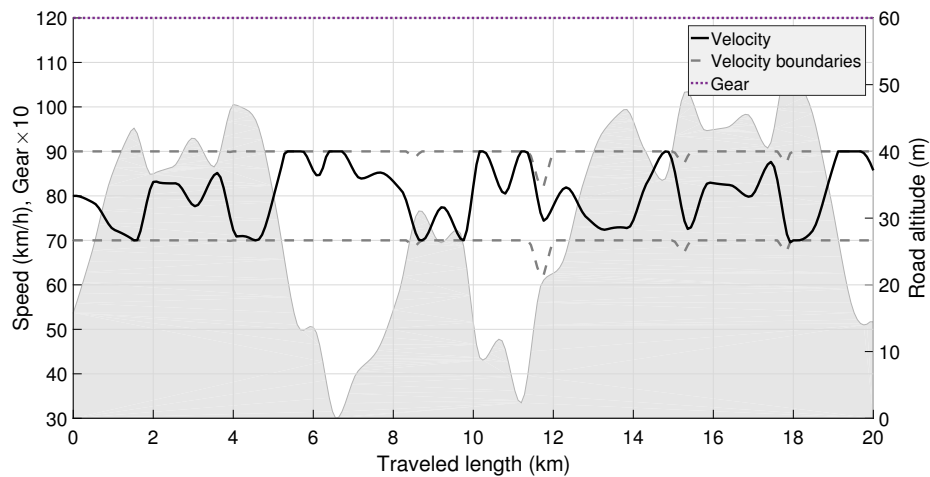


Figure 4.3: The velocity trajectory for a conventional vehicle with varying velocity as a function of traveled distance. The plot also shows the optimal gear choice.

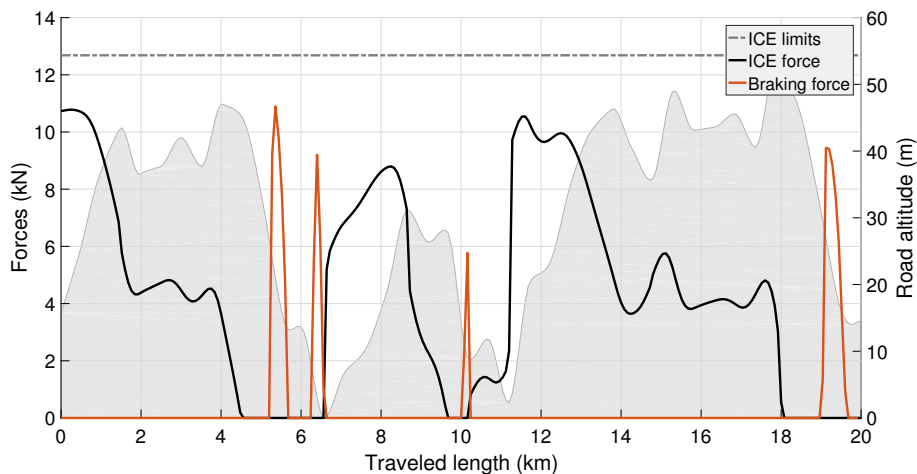


Figure 4.4: The forces acting on a conventional vehicle with varying velocity as function of traveled distance. The plot shows the optimal force from the ICE and the braking force.

The forces acting on the vehicle can be seen in Figure 4.4, where the force from the ICE along with the braking force is shown. Compared to Figure 4.2, less braking force is used in this case.

This is because now the energy can be stored as kinetic energy in the vehicle (by increasing the velocity) instead of wasting it by braking. Also note that braking is only used in the larger downhills when the velocity has reached its upper limit.

4.1.3 HEV with fixed velocity

The velocity trajectory along with the gear and ICE state trajectory are shown in Figure 4.5 for a single HEV with fixed velocity. The battery level in percentage (SOC) is also shown, which decrease in uphill (when the EM is used to power the vehicle) and increases in downhills (when the EM is used as a generator). The velocity profile is the same as in the conventional case. Note that the engine is off during the downhills of the driving cycle and that the gear remains the same all the time.

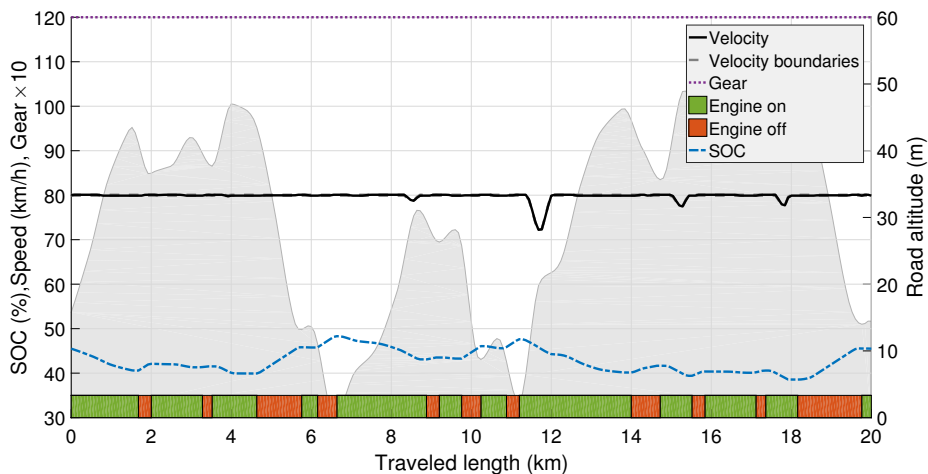


Figure 4.5: The velocity and SOC trajectories for an HEV with fixed velocity as a function of traveled distance. The plot also shows the optimal gear choice and ICE state.

The forces acting on the vehicle can be seen in Figure 4.6. The plot is similar as for the conventional vehicle case, but also includes the force from the EM along with its limits. In the uphill the EM force is positive to support the ICE. In the downhill the electric force is instead negative and is thereby charging the battery. Note that compared to the conventional vehicle (Figure 4.2), the hybrid to a large extent avoids wasting energy by using the mechanical brakes and instead stores the energy in the battery. The mechanical brakes are only used when the EM hits its limits.

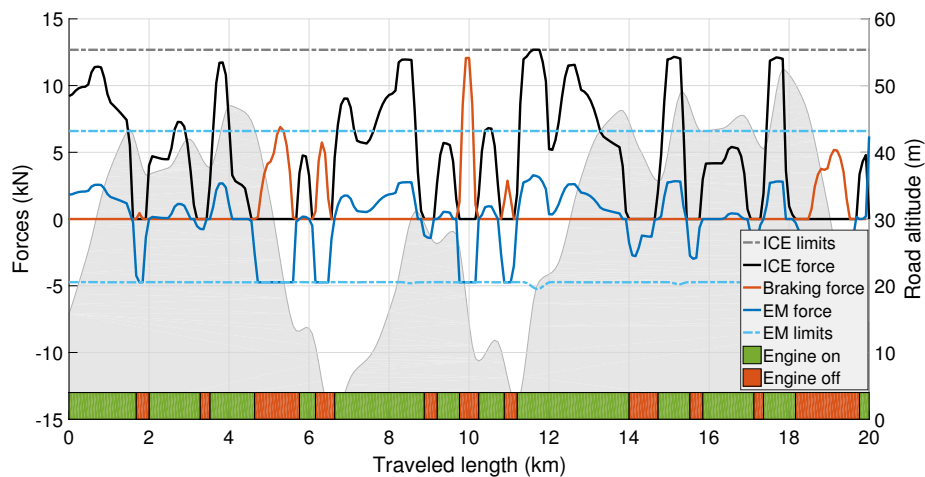


Figure 4.6: The forces acting on an HEV with fixed velocity as function of traveled distance. The plot shows the optimal force from the ICE, EM and the braking force. The ICE state is also presented.

4.1.4 HEV with varying velocity

The velocity trajectory along with the gear and ICE state trajectories are shown in Figure 4.7 for a single HEV with varying velocity. The battery level in percentage (SOC) is also shown which has similar behavior as the previous case. Some differences compared to Figure 4.5 is that the ICE has fewer state changes.

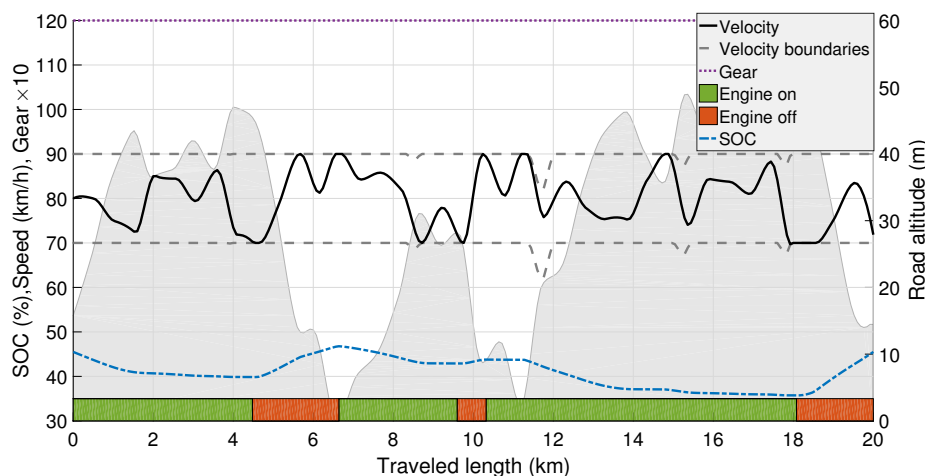


Figure 4.7: The velocity and SOC trajectories for an HEV with varying velocity as a function of traveled distance. The plot also shows the optimal gear choice and ICE state.

The forces acting on the vehicle can be seen in Figure 4.8. In this case, the force from the EM does not hit its limit that often, but most importantly no energy is wasted with the mechanical

brakes. This is achieved by allowing the velocity to increase and store the energy as kinetic energy, and when that is not possible, store it as electric energy in the battery instead.

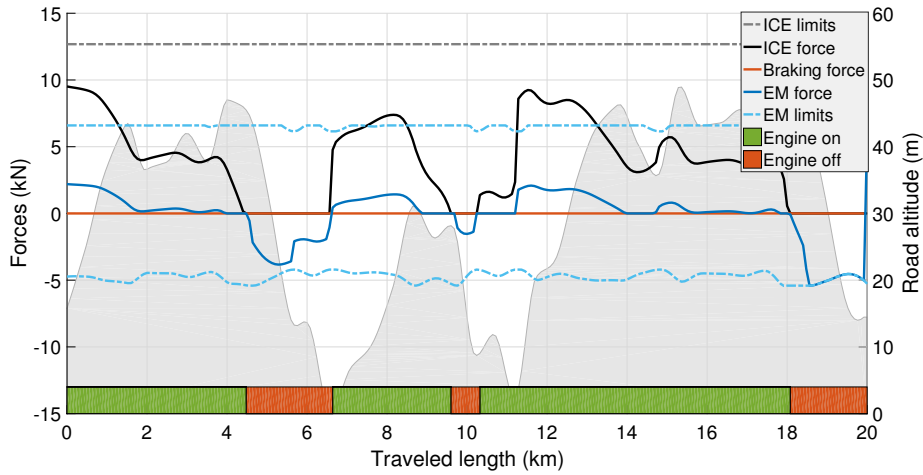


Figure 4.8: The forces acting on an HEV with varying velocity as function of traveled distance. The plot shows the optimal force from the ICE, EM and the braking force. The ICE state is also presented.

4.2 Case studies with multiple vehicles

For investigations with multiple vehicles, platoons up to the size of five vehicles (all homogeneous) are taken into consideration. Some results for conventional vehicles and HEVs in a 4-vehicle platoon can be seen in Figure 4.9 which shows the inter-vehicle distance, and in Figure 4.10 which shows the optimal velocity, gear and ICE state trajectories for all the vehicles in the platoon.

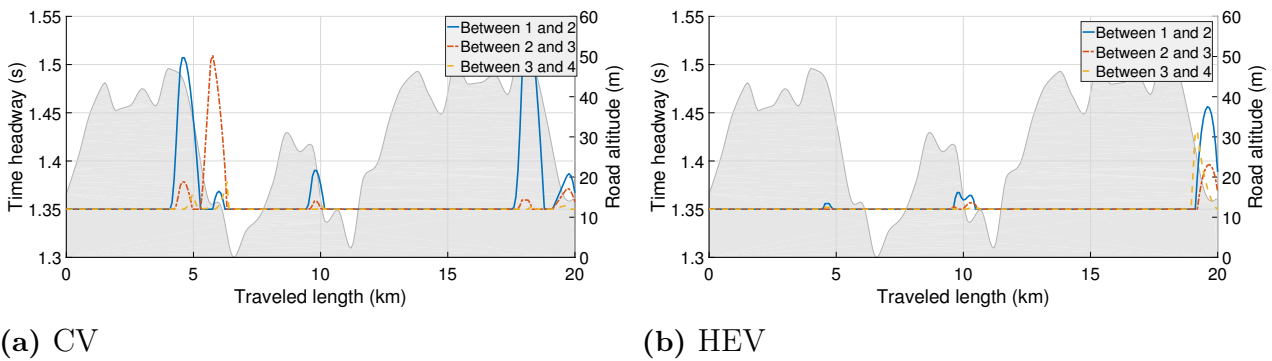


Figure 4.9: Inter-vehicle distance measured in time between the vehicles in a platoon consisting of four vehicles. The different lines represent the time distance between different vehicles, in this case 3 distances.

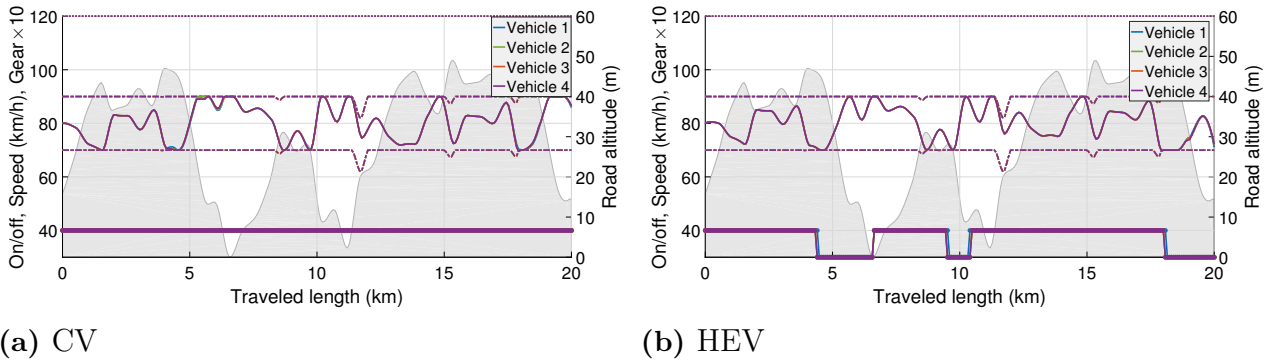


Figure 4.10: Velocity, gear and ICE status for all vehicles in a platoon of size four, plotted on top of each other.

For both the conventional and hybrid case, the inter-vehicle distances between the platoon members are mostly on the constraint for the minimum time-lag (which is 1.35 s in this case). It is only increasing in the downhills. This is because the trailing vehicles due to reduced air resistance would need to brake in the downhills to not hit the vehicles in front, if the minimum inter-vehicle distance is kept. Instead it is better for the trailing vehicles to stop using the engine a bit earlier before the downhill (than the vehicle in front) because they will catch up anyway. The HEVs will charge the battery as much as possible, but when no more energy can be put into the battery, they will behave as the conventional vehicles. Figure 4.10 is only included to show that all platoon members have a similar behavior regarding the velocity, gear and engine state. Note that the bottom line represents the ICE state (upper position means on) and that all the vehicles are plotted on top of each other. No force plots are presented here, because they look very similar to the single vehicle case.

The fuel consumption per vehicle for different types of vehicles and platoon sizes can be seen in Table 4.1. The chosen driving cycle is Borås-Landvetter-Borås which has a length of 86.9 km. As expected, HEVs are consuming less fuel than their conventional counterpart. Even HEVs with fixed velocity is consuming less fuel than conventional vehicles with varying velocity. There is also an improvement by increasing the size of the platoon, but the additional saving of fuel seems to get smaller for each vehicle added to the platoon. This applies for all vehicle types. As can be read from Table 4.1, the fuel consumption can be reduced by different approaches namely platooning vehicles, allowing the velocity to vary within an interval, or changing from conventional vehicles to HEVs. These approaches will now be presented in more details.

Table 4.1: Average fuel consumption per vehicle measured in l/100 km for different types of vehicles and platoon sizes. The number of vehicles in the platoon is represented by N .

N	CV fixed vel.	CV varying vel.	HEV fixed vel.	HEV varying vel.
1	32.83	29.18	28.84	26.80
2	31.75	28.01	27.53	25.42
3	31.11	27.34	26.73	24.57
4	30.79	27.00	26.34	24.16
5	30.60	26.80	26.10	23.91

4.2.1 Benefit of platooning

Due to reduction of air drag when driving in platoon, there are possibilities to save fuel by just letting several vehicles drive after each other. This is shown in Figure 4.11, where a comparison of the losses between an average platoon member and a single vehicle is plotted, for both the conventional and hybrid case.

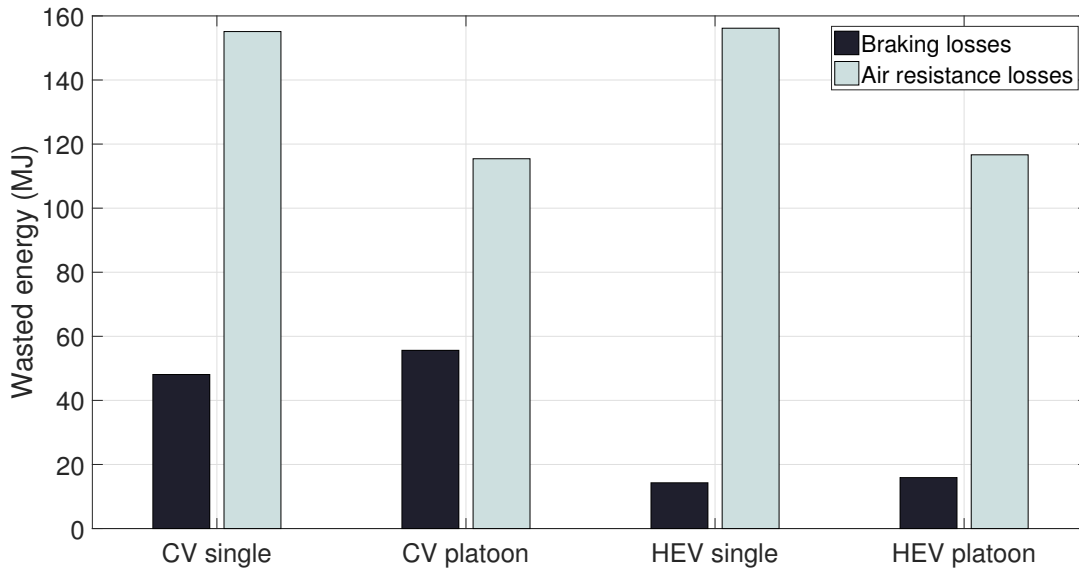


Figure 4.11: Comparisons of the losses from air resistance and braking forces between an average platoon member (of a platoon with four vehicles) and a single vehicle, both for conventional vehicle and HEV.

The platoon has four members and only the losses that show the biggest differences between the test cases are shown, which are the forces from the air resistance and the mechanical brakes. It can be seen that the platoon member has significantly lower losses than the single vehicle (both for conventional and platooning).

Figure 4.12 shows the reduction of fuel consumption for different platoon sizes in percentage, compared to the single vehicle counterpart for respective vehicle type. That is why the number of vehicles goes from 2 to 5. One interesting observation is that it seems to be more beneficial to make platoons of HEVs than of conventional vehicles. This can be understood by looking at Figure 4.11. The conventional platoon members have more mechanical braking losses than the single vehicle. This is because the trailing vehicles in the platoon experience less air resistance than the vehicles in front, and in the downhills they must therefore use the mechanical brakes to not run in to the vehicle in front. This behavior can be compared to the HEV case where almost no extra mechanical braking force have to be used. The HEV can brake using the EM and charge the battery instead.

Returning to Figure 4.12, when the velocity is allowed to vary, there is additional improvement when platooning compared to the case with fixed velocity for both conventional vehicles and

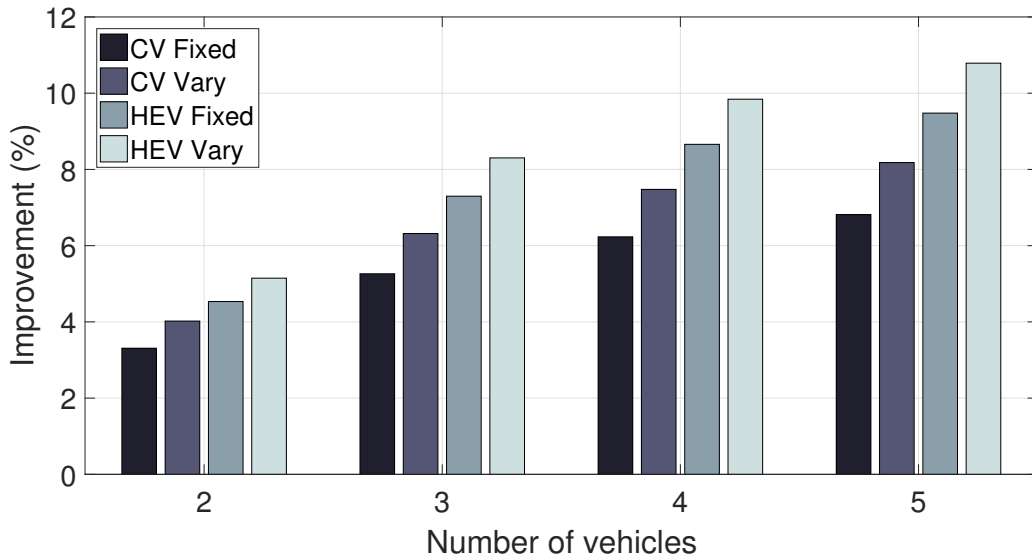


Figure 4.12: The improvement in average fuel consumption per vehicle of platooning from size 2 to size 5 for different types of vehicles compared to the fuel consumption for a single vehicle for respective type.

HEVs. This is probably because the air resistance is quadratic in velocity, which means that a vehicle which is varying its velocity will in total experience more losses, than a vehicle that keeps a constant velocity. Because of this, vehicles with varying velocity have more to gain by platooning than vehicles with constant velocity. It is also shown from Figure 4.12 that platooning is more beneficial for HEVs with fixed velocity than for conventional vehicle with varying velocity.

4.2.2 Benefit with varying velocity

Less usage of braking can be achieved by allowing the velocity to vary for the vehicles, and thereby saving fuel. The improvement from having fixed velocity to varying for different platoon sizes is shown in Figure 4.13, where the reduction of fuel for both conventional vehicles and HEVs are presented. The conventional vehicles gain more improvement for allowing the velocity to vary rather than having a fixed one compared with HEVs. This is because conventional vehicles are able to reduce much more braking force, since HEVs are primarily storing energy in the battery there is less braking force to begin with, and thereby less potential of improvements. The improvements are also increasing with the size of the platoon, but it seems that lesser additional improvements are gained when increasing the platoon size further.

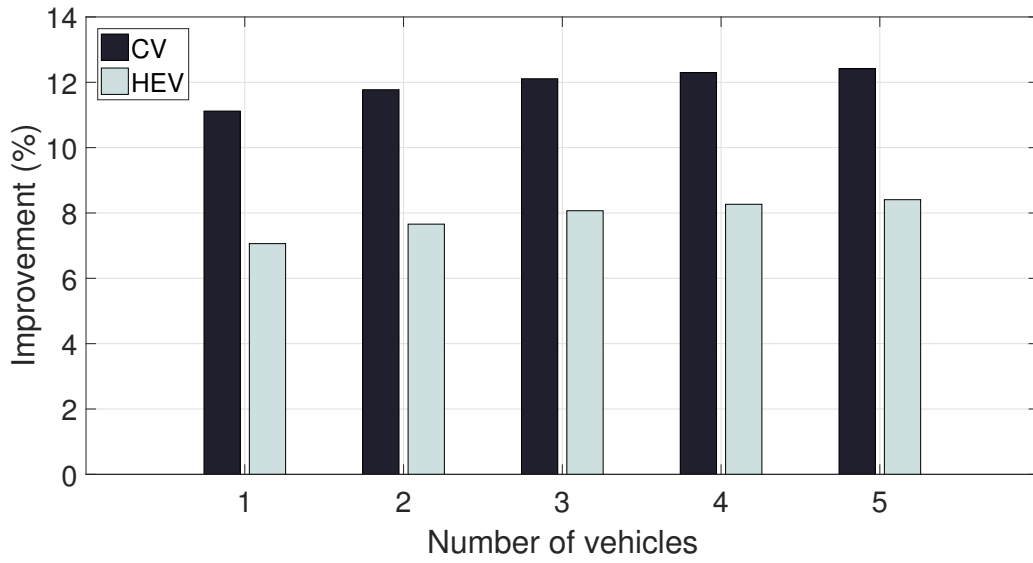


Figure 4.13: The improvement in average fuel consumption per vehicle of allowing the velocity to vary within an interval compared of having a fixed velocity. Both conventional vehicles and HEVs in platoons up to size 5 are presented.

4.2.3 Benefit with HEV

As expected it is possible to save fuel by using HEVs instead of conventional vehicles, otherwise it would not be any point to invest resources into this topic. The reason behind this is already

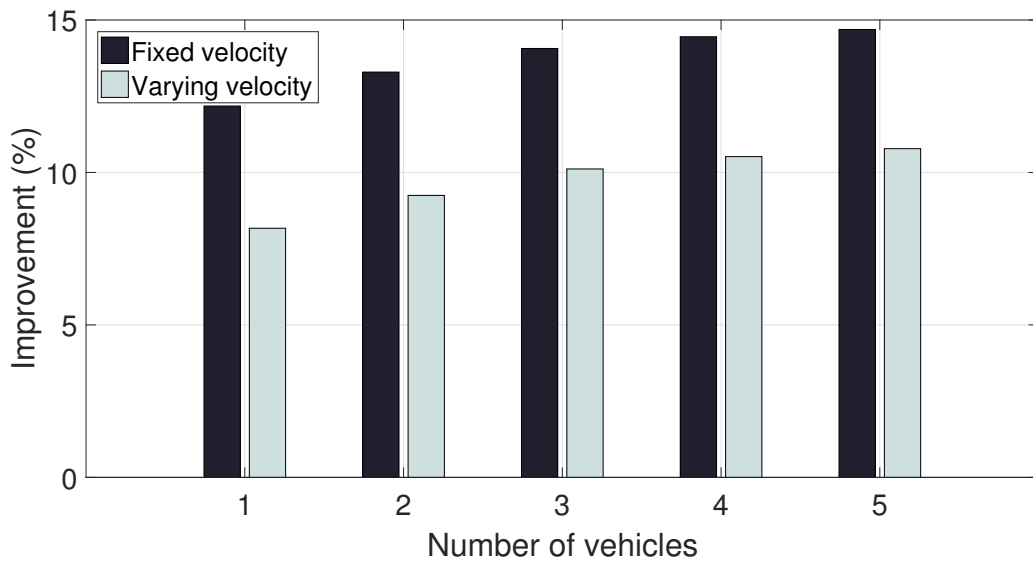


Figure 4.14: The improvement in average fuel consumption per vehicle when comparing conventional vehicles with HEVs of the same platoon size. Both vehicles with fixed and varying velocity in platoons up to size 5 are presented.

discussed for the single vehicle case, and once again has to do with the fact that less energy has to be wasted on braking. The reduction of fuel consumption by changing from conventional vehicles to HEVs can be seen in Figure 4.14 for different platoon sizes, where the improvement of having fixed velocity varying velocity are presented. The vehicles with fixed velocity are gaining more benefits by using HEVs than the vehicles with varying velocity. As similar to previous results, there is less additional improvement gaining for increasing the platoon size even further.

4.3 Special investigations

This section presents some special investigations, where other effects other than platooning and vehicle type are taken into consideration. These investigations are about how to order the vehicles when the platoon is consisting of a mixture of conventional vehicles and HEVs, and how the velocity variation and reduced air resistance are affecting the fuel consumption.

4.3.1 Mixed platoon of conventional vehicles and HEVs

Previous results only considered homogeneous platoons where each individual vehicle in the platoon had exactly the same properties. By allowing the platoon to consist of a mixture of conventional vehicles and HEVs, the result depends of how the vehicles are ordered. Here the case with a platoon consisting of four vehicles, where two of them are conventional and two are hybrid (otherwise identical) is investigated. There are 6 combination when ordering 2 vehicles among 4 vehicles. The result for all different combinations is shown in Table 4.2, where crossed boxes represent the positions of the conventional vehicles in the platoon driving to the right. Least fuel is used when the conventional vehicles are positioned in the front of the platoon. The reason for this is that conventional vehicles cannot fully utilize the reduction of air drag when being positioned at the middle or the rear of the platoon. To avoid driving too close to the vehicle ahead, it either needs to brake or increase the inter-vehicle distance. The HEVs have on the other hand the opportunity to put the excess energy in the battery instead. Therefore, less fuel is used when the conventional vehicles are driving first.

Table 4.2: Average fuel consumption per vehicle when there are 2 conventional vehicles and 2 HEVs in a platoon. The position of the conventional vehicles in the platoon is marked with \boxtimes , and the platoon is driving to the right.

Position	Fuel consumption (l/100 km)	Percentage of the minimum consumption (%)
$\square \square \boxtimes \boxtimes$	24.89	100.00
$\square \boxtimes \square \boxtimes$	24.94	100.23
$\boxtimes \square \square \boxtimes$	24.91	100.09
$\square \boxtimes \boxtimes \square$	25.07	100.72
$\boxtimes \square \boxtimes \square$	25.04	100.60
$\boxtimes \boxtimes \square \square$	25.08	100.80

4.3.2 Velocity variation

By allowing the velocities of the vehicles to vary within a specific interval $\pm\Delta_v$, there is an opportunity to store kinetic energy in the vehicles. Depending on the size of this interval, the reduction in fuel consumption becomes different. The case with a 4-vehicle platoon is solved for different allowed velocity intervals and the comparison between a platoon of conventional vehicles and a platoon of HEVs can be seen in Figure 4.15. The improvements of the fuel consumption are with respect to the fixed velocity case of respective vehicle type. The result is heavily affected by how hilly the terrain is for the used driving cycle.

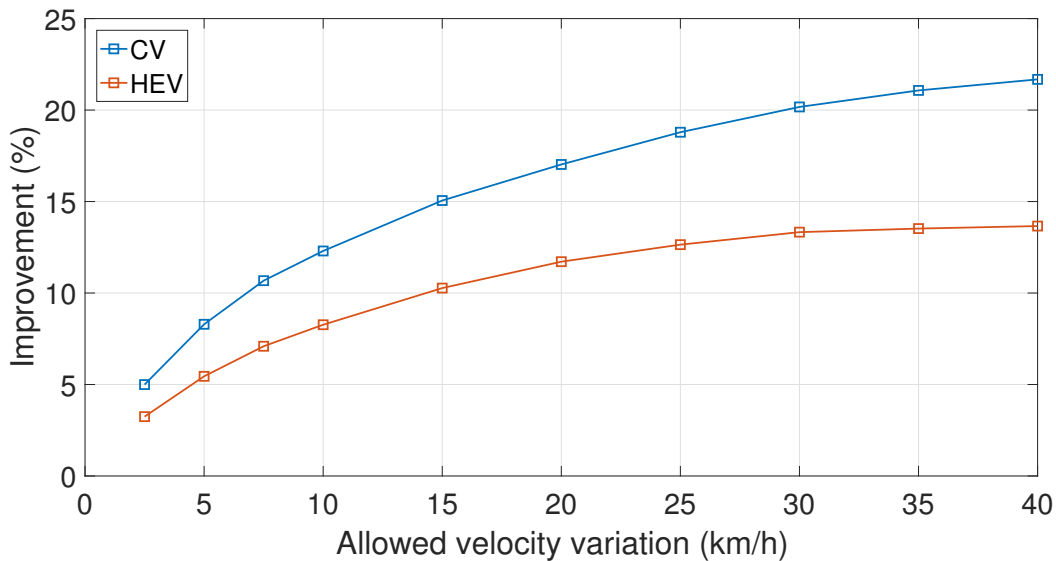


Figure 4.15: The improvement in average fuel consumption per vehicle for conventional vehicles and HEVs in a 4-vehicle platoon for different sizes of the allowed velocity interval Δ_v compared to having a fixed velocity for the platoon.

The effect of increasing the interval of allowed velocity variation is affecting the conventional vehicles more than the HEVs. For the HEVs, the improvements seem to flatten out by at around 14%, while the conventional case still seems to gain some improvements even beyond a velocity variation of ± 40 km/h. The reason for this behavior has a lot to do with the usage of braking force. With increasing velocity gap, the HEVs can avoid to brake and instead store the energy in the battery or as kinetic energy. With a velocity variation of about ± 30 km/h and onward the HEVs are not using any braking force and thereby not continuing to increase its improvement. The conventional vehicles do not have the option to store energy in a battery and will entirely use braking to dispose surplus energy. By increasing the allowed velocity gap, more energy can be stored as kinetic energy and less braking force is needed. Unlike the HEVs, the conventional vehicles are still using braking forces at a velocity variation of ± 40 km/h due to the absence of a battery. That is the reason why the conventional vehicles are gaining much more improvement with respect to velocity gap than the HEVs. By just allowing velocity variance of ± 5 km/h, there is around 8% improvement for a conventional vehicle and 5% for an HEV, and it is probably not even noticeable by the driver. More details regarding the fuel

consumption and the improvements can be found in Table C.1 in Appendix C.

4.3.3 Reduced air drag coefficient

The air resistance the vehicles are experiencing depends on the velocity, air density, frontal area and the aerodynamic constant, see equation (2.2). In the previous case studies, the aerodynamic constant c_d has a value of 0.6, which is a typical value for trucks. In this subsection some comparisons are made between the case with an aerodynamic coefficient of 0.6 and the case with an aerodynamic coefficient of 0.3, which is a typical value for cars. The data from these comparisons are presented in Table C.2 in Appendix C, where also Figure C.2 can be seen showing the velocity profiles for the two different cases. The velocity profiles are not affected significantly by the difference in air resistance. It is also worth mentioning that the distances between the vehicles are not affected significantly either, even if no figures are presented to show this.

With a lower air resistance, less fuel are consumed in general for all different kinds of platoons. However, what is most interesting is how the improvement in fuel consumption between different vehicle configurations are affected by the air resistance. In Table 4.3, the percentage improvement in fuel using HEVs in a 4-vehicle platoon is presented for the two different air drag coefficients. First of all, it is more to gain by platooning when the air resistance is high. This is because, the higher the air resistance is the higher the losses are. Therefore, there is more fuel to save by reducing these losses for the case with high air resistance compared to the case with low air resistance. It can also be seen that the gain of changing from conventional vehicles to HEVs becomes larger for a lower value of c_d . The reason behind the increased improvement is that the force from the EM makes up a larger part of the total force from both the ICE and the EM and since the fuel consumption is quadratic in force the improvement gets bigger.

Table 4.3: Improvement in average fuel consumption per vehicle for different air drag coefficients. The comparisons are made between a single HEV vs a 4-vehicle platoon of HEVs and between a 4-vehicle platoon of conventional vehicles vs a platoon of HEVs with the same size.

c_d	Improvement (%)	
	HEV: platoon (of 4) vs single	platoon (of 4): HEV vs CV
0.6	9.8	10.5
0.3	6.2	15.1

4.3.4 Reduced mass

In all the previous test cases the vehicles had a mass of 41.8 t. In this subsection, some test cases are made with a platoon consisting of vehicles with a mass of 18.5 t, which is roughly the mass of a vehicle with no load. Table C.3 in Appendix C, the data from these case studies is presented, where also Figure C.1 can be seen showing the velocity profiles of the vehicles for the two different platoons. From the figure it can be seen that the velocity profiles for the

heavy vehicles are varying a lot more around the reference speed than for the light vehicles. It is also worth mentioning that the distance between the vehicles does not seem to be affected significantly by the different masses.

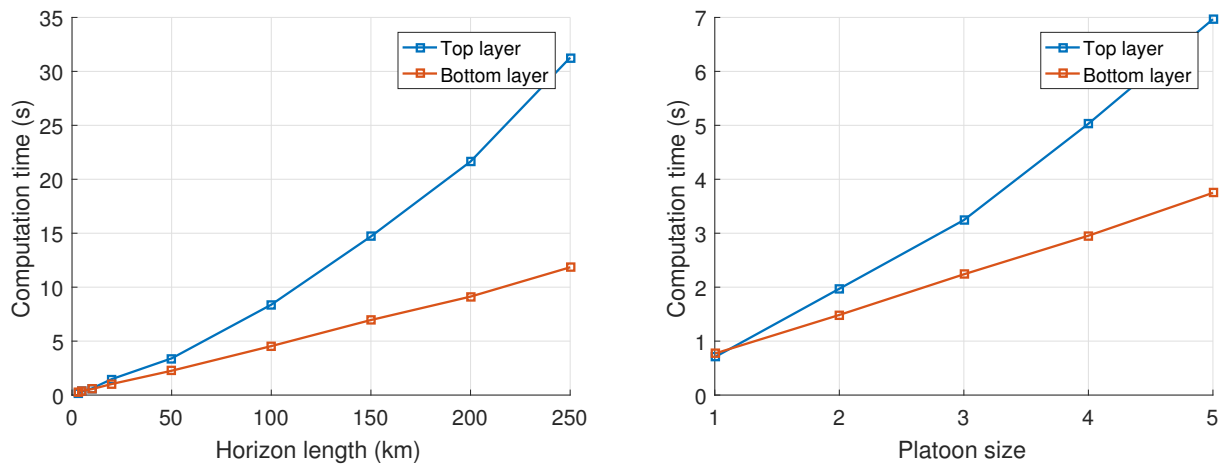
In Table 4.4, a comparison is made between the two different cases, regarding how much improvements that can be made by platooning with HEVs. First of all it seems like it is more to gain by platooning with lighter vehicles. This is because the losses due to air resistance is a bigger part of the total losses for the lighter vehicles compared to the heavier ones. Therefore, there are more improvements in percentage to be made with the lighter vehicles. It also seems like it is more to gain by platooning when the vehicles are heavy. This is because the heavier the vehicles are, the more energy is wasted with the conventional vehicles on braking, and therefore there are more potential for improvements with HEVs.

Table 4.4: Improvement in average fuel consumption per vehicle for different masses. The comparisons are made between a single HEV vs a 4-vehicle platoon of HEVs and between a 4-vehicle platoon of conventional vehicles vs a platoon of HEVs with the same size.

Mass (t)	Improvement (%)	
	HEV: platoon (of 4) vs single	platoon (of 4): HEV vs CV
41.8	9.8	10.5
18.5	14.4	7.0

4.4 Computation time performance

The computation times for the top layer (SOCP) and bottom layer optimization (DP) are presented in Figure 4.16. In Figure 4.16a the relationship between computation time and horizon length are investigated. It seems like the relationship is linear for the DP and quadratic or exponential for the SOCP. Similar results can be found in Figure 4.16b, where the computation time is plotted over platoon size. Once again, the relationship is linear for the DP and quadratic or exponential for the SOCP. This behavior is reasonable since the DP is done separately for each of the vehicles, while the SOCP is done for the whole platoon. In Figure 4.17 the total computation time of the control algorithm is presented, which includes several iterations of the top and bottom layers. Not surprisingly, the trend seems to be quadratic here as well. The big variance in the computation time is probably because the computations are done on a standard PC, which is not deterministic. For a short horizon of 5 km the computation takes around 1.9s. This means that the computation is done before the next sample, which is desired if this control strategy is to be used in an MPC-scheme. This comparisons are of course not completely relevant for the case with real vehicles, since different hardware and software would be used, but the results are still promising.



(a) Computation time over horizon length for a platoon with four vehicles. (b) Computation time over number of vehicles in the platoon, with an horizon of 86.9 km.

Figure 4.16: Average computation time on a standard PC (Intel Core i5-2450M 2.5 GHz and 4 GB RAM), for one iteration of each of the two optimization layers as a function of horizon length and platoon size. The computation time for the top layer seems to increase quadratic or exponential with both those things, while for the lower layer the increment is linear.

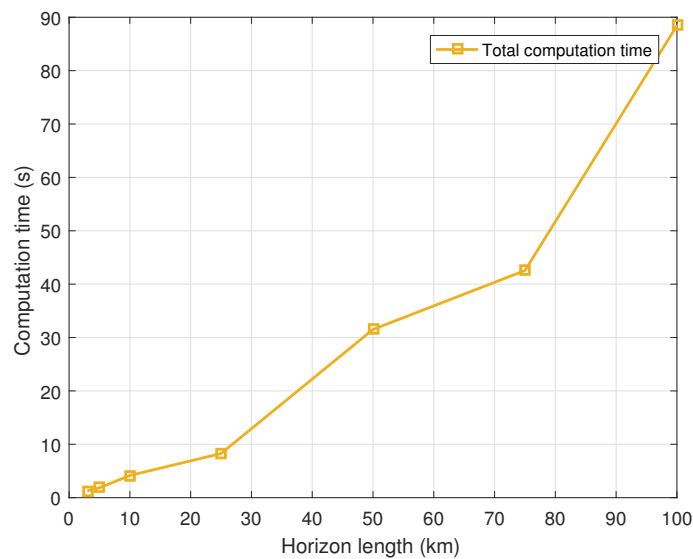


Figure 4.17: Total computation time of the control algorithm with a platoon of four vehicles as a function of horizon length. The computations are done on a standard PC (Intel Core i5-4200U 2.30 GHz and 8 GB RAM).

5

Discussion

This chapter discuss the results presented in the previous chapter. Discussions regarding the models and the optimization algorithm is also included as well as some sustainability and ethical aspects connected to the outcome of the project.

5.1 Validity of the models and results

All the simplifications applied to the problem are affecting the validity of the results. One simplification is to divide the optimization problem into two layers to avoid mixed real and integer formulations. There is then the possibility of model mismatch between the layers, since for example the top layer is using the reference velocity/kinetic energy as linearization point, while the bottom layer is using the velocity directly. However, the most essential modelling aspects are still included in the formulations, like not having constant efficiency of the ICE and EM, and that the loss functions are nonlinear.

No serious attempts have been made to verify that the solutions of the controller really are the optimal ones. However, it is worth mentioning that in [13], they do verify the control algorithm by comparing it to an exact solution, that is found using DP. The result shows that the controller does find the optimal solution. The control algorithm used in this project is very similar to the one used in [13], so at least the principal is sound. However, they did not consider HEVs which of course could change the result significantly. If the controller in this project would be verified, the method of choice would probably also be to compare it with an exact solution obtained with DP. This would however be very computational demanding.

In the bottom layer, it is not allowed to use the ICE when the demanded force is negative and the EM acts like a generator. This is not because of physical limitations on the engine, but rather to make it easier to solve the power split. However, there might be scenarios where it is beneficial to do so. For example, during a downhill when the EM does not hit its lower constraint and it is possible to convert energy from the ICE to the battery. The extra energy in the battery can later be used in uphill to reduce the use of the ICE. Since the losses are quadratic it is more profitable to use small forces during a long interval than to use large forces during a short interval.

The comparison between a conventional vehicle and a hybrid vehicle is not straight forward. In the comparisons in this project, the same ICE is used for both conventional vehicles and HEVs, which means that HEVs can utilize more power with the addition of the EM. The total power from the engines is thereby different for the two vehicle types. In reality the ICE implemented in the HEVs might be slightly weaker so the total power is about the same for both types. It is also worth mentioning that while driving without load, the HEVs are slightly heavier than conventional vehicles due to the inclusion of the battery and the EM. This implies that the HEVs transport less goods compared with conventional vehicles when the same total mass is used for both types of vehicles as presented in the results. This effect is for simplicity not taking into consideration when making comparisons between the vehicles, even though it would be more correct.

5.2 Sustainability and ethical aspects

It has already been mentioned in the introduction that fuel costs is a large part of trucking companies expenditures [2]. The test cases have shown that the designed controller have the potential so significantly lower the fuel consumption of moving vehicles, and thereby contributing to economical sustainability. Furthermore, this project can be seen as a part in a more general development in the automotive industry, towards self-driving vehicles. This have the potential to remove a lot of jobs in the transportation business in the coming years [22], which could also contribute to economical sustainability. Another conclusion from [2] was that on average 35 % of the expenditures for trucking companies are labor wages and benefits. This means that there a lot of money to be saved if no drivers are needed.

The question is if this potential loss of jobs is ethically and socially sustainable or not. A recent study published in the American Journal of Industrial Medicine [23] shows that truck drivers compared to the general population, are more exposed to negative health effects such as obesity, lack of physical activity and lack of sleep. With this in mind it may be argued that it is socially sustainable to remove the job as a driver, making it possible for people to spend their time on something else. On the other hand, the direct effect for people losing their job may of course be negative. Especially if they are old and with no other education, it may be difficult to find a new job.

The potential reduction of fuel also contributes to ecological sustainability. Less fuel consumption means less diesel emissions, which is known to have several negative effects on human health and the environment. Diesel emissions can cause cancer [24], and it contributes to global warming as well as pollution of air and water [25].

6

Conclusion

In this project the dynamics of a platoon consisting of HEVs, have been modelled and a control algorithm capable of minimizing the fuel consumption for such a platoon have been designed. The models include mathematical formulations of the ICE, EM, battery, gearbox and air resistance, as well as the differential equations of the vehicle dynamics and mechanical- and electrical power balance.

Using these models an optimization problem has been formulated, and a control algorithm has been designed, which divides the optimization into two layers. The top layer handles the velocity and is solved by simplifying the mathematical formulations and using convex optimization. The bottom layer handles the gear and ICE state and is using DP.

The control algorithm uses three approaches to save fuel. One is to use information of the topography of the road ahead, to plan the speed of each of the vehicles, and thereby avoid using the mechanical brakes. Another one is to save excess kinetic energy of the vehicle as electric energy in the battery to be used for later. The last one is to have the trucks drive close after one another to reduce the air resistance.

The control strategy has been tested and applied in case studies, both for the case with a single vehicle, to show the functionality of the algorithm, but also for the case with multiple vehicles. For the case with multiple vehicles several tests have been performed with different vehicle configurations to see how platooning, varying velocity and hybridization are affecting the fuel consumption. For the case with platooning, results show that up to 10 % can be saved for an HEV traveling in a platoon of 4 vehicles compared to on its own. For the case with hybridization, up to 11 % can be saved when using a platoon of hybrid vehicles compared to a platoon of conventional vehicles if they both drive with the optimal velocity. Finally, the performance of the algorithm have been investigated, which showed that the computation time is below 2 s for an horizon of 5 km.

7

Future Work

The controller is mainly designed to use in simulations. If it is to be used for real vehicles, more work needs to be done. For example, on a real vehicle there will be model mismatches between the models that are used in the controller and the actual dynamics of the vehicle. This may require the addition of another control layer similarly as to what is presented in [15]. Furthermore, the control algorithm may need to be simplified to enable faster computation. One possibility would be to simplify the optimization formulations (3.28) and (3.29) to make them suitable for a QP problem. Another problem that needs to be handled when using real vehicles is to find a preferable horizon length for the MPC. In this project, the horizon is the entire driving cycle, and the optimization is only done once for the entire horizon. This works because no disturbances are considered. For real vehicle, the horizon would be shorter and the optimization would be done more often. However, for the energy management of the battery to be meaningful, the horizon cannot be too short.

Another possibility for future work is to do more case studies. There is a large amount of combinations of vehicle configurations to test. In this project, only a few of the most interesting test cases have been made, but there are other tests and comparisons that could be interesting as well, for example comparing different masses and engine power. The case studies could also be more detailed. For example, include disturbances or to model the communication delay that exists when using V2V communications. It would be interesting to see if these modifications would have any significant impact on the results.

It is only considered that the vehicles are driving in highway speed without any other surrounding vehicles. It may be useful to look at other environments as well, for example a city environment, where the speed is much lower and starts and stops occur due to traffic lights for example.

One important aspect to take into consideration when platooning is the ordering of the vehicles. With the controller used in this project, the order of the vehicles is fixed. It would be useful if the controller itself could find the optimal ordering of the vehicles. Maybe even allow overtaking to be able to use different ordering for different parts of the driving cycle as this may be the optimal solution. However, this would probably be very computational demanding.

The vehicle models that have been used can be made more detailed. Perhaps most relevant is to model the engine braking. In the controller that has been used in this project, there is no difference between braking with the brakes or with the engine. However, with a real vehicle it

is preferred to avoid using the brakes, to reduce the wear on them. Another aspect that has a lot of room for improvements is the air drag, which is rather complex to model, and the models that are used are very simplified. For example, the data that are used to create the models comes from a platoon with three vehicles with equal inter-vehicle distances. In the simulations, the inter-vehicle distances may vary, and the platoons consists of more than three vehicles. Additionally, the air drag model that is used assumes that there is no crosswind, which could have a huge impact on the air resistance.

Finally, the controller optimizes the energy consumption of the entire platoon as a whole. It is perhaps too optimistic to assume that real drivers and companies would cooperate this nicely. If each vehicle would do their optimization separately, the result regarding fuel consumption would probably be worse. However, it would still contribute to the progress of making transportation more efficient and sustainable.

Bibliography

- [1] Volvo Trucks, *Volvo concept truck*. [Online]. Available: <http://www.volvotrucks.com/en-en/home.html> (visited on 05/17/2017).
- [2] “An analysis of the operational costs of trucking: 2015 update”, American Transportation Research Institute, Tech. Rep., 2015.
- [3] European Environment Agency, *Outdoor air quality in urban areas*. [Online]. Available: <https://www.eea.europa.eu/airs/2016/environment-and-health/outdoor-air-quality-urban-areas> (visited on 05/11/2017).
- [4] Eurostat, *Greenhouse gas emission statistics*. [Online]. Available: http://ec.europa.eu/eurostat/statistics-explained/index.php/Greenhouse_gas_emission_statistics (visited on 05/17/2017).
- [5] S. Björnander and L. Grunske, “Adaptive cruise controllers – a literature review”, Faculty of Information and Communications Technologies, Tech. Rep., Aug. 2008.
- [6] V. Milanés, S. E. Shladover, J. Spring, C. Nowakowski, H. Kawazoe, and M. Nakamura, “Cooperative adaptive cruise control in real traffic situations”, *IEEE Transactions on Intelligent Transportation Systems*, vol. 15, pp. 296–305, Feb. 2014.
- [7] E. Hellström, J. Åslund, and L. Nielsen, “Design of an efficient algorithm for fuel-optimal look-ahead control”, *Control Engineering Practice*, vol. 18, pp. 1318–1327, 2010.
- [8] E. F. Camacho and C. Bordons, *Model Predictive control*. Springer London, 2007.
- [9] R. Bellman, *Dynamic Programming*. Princeton University Press, 1957.
- [10] M. Diaby and A. Sorkati, “Optimization for energy efficient cooperative adaptive cruise control”, Master’s thesis, Chalmers University of Technology, Gothenburg, 2016.
- [11] M. Jeber, “A moving horizon predictive controller for truck platoons”, Master’s thesis, Chalmers University of Technology, Gothenburg, 2015.

- [12] J. Wahnström, “Energy optimization for platooning through utilizing the road topography”, Master’s thesis, Lund University, Lund, 2015.
- [13] N. Murgovski, B. Egardt, and M. Nilsson, “Cooperative energy management of automated vehicles”, *Control Engineering Practice*, vol. 57, pp. 84–98, 2016.
- [14] A. Sicarretta and L. Guzzella, “Control of hybrid electric vehicles”, *IEEE Control Systems Magazine*, pp. 60–70, Apr. 2007.
- [15] L. Johannesson, N. Murgovski, E. Jonasson, J. Hellgren, and B. Egardt, “Predictive energy management of hybrid long-haul trucks”, *Control Engineering Practice*, vol. 41, pp. 83–97, 2015.
- [16] CVX Research, *Matlab software for disciplined convex programming*. [Online]. Available: <http://cvxr.com/cvx/> (visited on 01/16/2017).
- [17] S. Boyd and L. Vandenberghe, *Convex Optimization*, 7th ed. Cambridge University Press, 2004.
- [18] J. Renegar, *A Mathematical View of Interior-Point Methods in Convex Optimization*, 1st ed. Society for Industrial and Applied Mathematics, 2001.
- [19] E. D. Andersen, D. Jensen, J. Jensen, R. Sandvik, and U. Worsøe, “Mosek version 6. mosek technical report: Tr-2009-3”, Tech. Rep., Oct. 2009.
- [20] D. S. Naidu, *Optimal Control Systems*. CRC Press, 2002.
- [21] Wikipedia, *Quartic functions*. [Online]. Available: https://en.wikipedia.org/wiki/Quartic_function (visited on 04/03/2017).
- [22] A. Balakrishnan, *Self-driving cars could cost america’s professional drivers up to 25,000 jobs a month, goldman sachs says*. [Online]. Available: <http://www.cnbc.com/2017/05/22/goldman-sachs-analysis-of-autonomous-vehicle-job-loss.html> (visited on 05/26/2017).
- [23] W. K. Sieber, C. F. Robinson, J. Birdsey, G. X. Chen, E. M. Hitchcock, J. E. Lincoln, A. Nakata, and M. H. Sweeney, “Obesity and other risk factors: The national survey of u.s. long-haul truck driver health and injury”, *American Journal of Industrial Medicine*, vol. 57, no. 6,
- [24] I. W. G. on the Evaluation of Carcinogenic Risks to Human, *Diesel and gasoline exhausts and some nitroarenes*, ser. IARC Monographs on the Evaluation of Carcinogenic Risks to Humans. International Agency for Research on Cancer, 2012, vol. 105.
- [25] A. Lloyd and T. Cackette, “Diesel engines: Environmental impact and control”, *J Air Waste Manag Assoc*, vol. 51, no. 6, pp. 809–47, 2001.

A

Model Parameters

Table A.1: Values of the model parameters that are used in the case studies.

Parameter	Notation	Value	Unit
Aerodynamic drag coefficient	c_d	0.6	-
Air density	ρ_a	1.1839	kg/m ³
Auxiliary power	P_A	1.6	kW
Battery open voltage	V_{oc}	637	V
Battery resistance	R	0.173	Ω
Cruising velocity	\bar{v}	80	km/h
Frontal area	A_f	10.2	m ²
Gear efficiency (including differential gear)	η	0.9506	-
Gravitational acceleration	g	9.81	m/s ²
Highest gear	γ_{\max}	12	-
Maximum acceleration	a_{\max}	0.2	m/s ²
Maximum battery charging power	$P_{B\max}$	100	kW
Maximum battery energy capacity	$E_{B\max}$	19	kWh
Maximum EM power	$P_{M\max}$	180	kW
Maximum ICE power	$P_{E\max}$	350	kW
Maximum SOC level	SOC_{\max}	0.65	-
Minimum SOC level	SOC_{\min}	0.20	-
Penalty for gear change	w_γ	0.00005	kg/s
Penalty for ICE on/off	w_χ	0.0007	kg/s
Rolling resistance coefficient	c_r	0.0047	-
Vehicle mass	m	41.8	t
Wheel radius	R_w	0.491	m

B

Pre-filter to Obtain Feasible Reference Speed

A pre-filter similar used in [13] is applied before the start of the optimization algorithm to obtain a reference velocity $\hat{v}(s)$ from the chosen cruising speed \bar{v} , speed limits $v_{\min}^{\text{road}}(s)$, $v_{\max}^{\text{road}}(s)$ and the road information for the driving cycle. Note that the variables are expressed in the space coordinate s . It is assumed that $\bar{v} \in [v_{\min}^{\text{road}}(s), v_{\max}^{\text{road}}(s)]$ and $\forall s \in [0, s_f]$.

The maximum net force that can be delivered to the wheels by the ICE at gear γ for a single vehicle at velocity $\hat{v}(s)$ can be expressed as

$$F_{W\max}(\hat{v}(s), \gamma) = F_{E\max}(\hat{v}(s), \gamma) - F_{\text{air}}^o(\hat{v}(s)) - mg(\sin(\alpha(s)) + c_r \cos(\alpha(s))). \quad (\text{B.1})$$

Only the force from the ICE is considered and not from the electric machine so the comparisons between conventional vehicles and HEVs becomes more fair. The reference velocity is obtained by numerically solving

$$\hat{v}(s) = \min \left\{ \bar{v}, \int_0^{s_f} \min \left\{ \frac{a_{\max}}{\hat{v}(s)}, \max_{\gamma} \left\{ \frac{F_{W\max}(\hat{v}(s), \gamma)}{m_e \hat{v}(s)} \right\} \right\} ds \right\}, \quad (\text{B.2})$$

where a_{\max} is the maximum acceleration that is allowed in order to experience a comfortable drive. The initial condition is $\hat{v}(0) = \bar{v}$. If it happens that $\hat{v}(s) < v_{\min}^{\text{road}}(s)$ for some instances s , the limit has to be modified accordingly to avoid infeasibility. The velocity limits used in the algorithm are calculated as

$$\begin{aligned} v_{\min}(s) &= \max \left\{ v_{\min}^{\text{road}}(s), \hat{v}(s) - \Delta_v \right\}, \\ v_{\max}(s) &= \min \left\{ v_{\max}^{\text{road}}(s), \hat{v}(s) + \Delta_v \right\}, \end{aligned} \quad (\text{B.3})$$

where Δ_v is the maximum allowed speed variation from the reference speed. The maximum traveling time T_{\max} is obtained from the reference speed according to

$$T_{\max} = \int_0^{s_f} \frac{1}{\hat{v}(s)} ds. \quad (\text{B.4})$$

C

Additional Details from Case-studies

Table C.1: Improvement in fuel consumption (l/100 km) per vehicle for a platoon of 4 vehicles compared to a single vehicle for different allowed velocity intervals. Each vehicle type (CV and HEV) are compared to their own single vehicle type.

Interval (km/h)	4 HEV (l/100 km)	Improv (%)	4 CV (l/100 km)	Improv (%)
0	26.34	0	30.79	0
2.5	25.49	3.243	29.25	4.996
5	24.90	5.447	28.24	8.291
7.5	24.47	7.091	27.50	10.67
10	24.16	8.267	27.00	12.30
15	23.63	10.27	26.15	15.06
20	23.25	11.71	25.55	17.03
25	23.01	12.64	25.00	18.79
30	22.83	13.33	24.58	20.17
35	22.78	13.52	24.30	21.07
40	22.74	13.66	24.11	21.68

Table C.2: Average fuel consumption per vehicle for a 4-vehicle platoon of conventional vehicles and HEVs and for a single HEV, for different values of the aerodynamic constant c_d .

c_d	4 CV (l/100 km)	4 HEV (l/100 km)	1 HEV (l/100 km)
0.6	27.00	24.16	26.80
0.3	23.98	20.36	21.71

Table C.3: Average fuel consumption per vehicle for a 4-vehicle platoon of conventional vehicles and HEVs and for a single HEV, for different masses.

Mass t	4 CV (l/100 km)	4 HEV (l/100 km)	1 HEV (l/100 km)
41.8	27.00	24.16	26.80
18.5	17.73	16.48	19.26

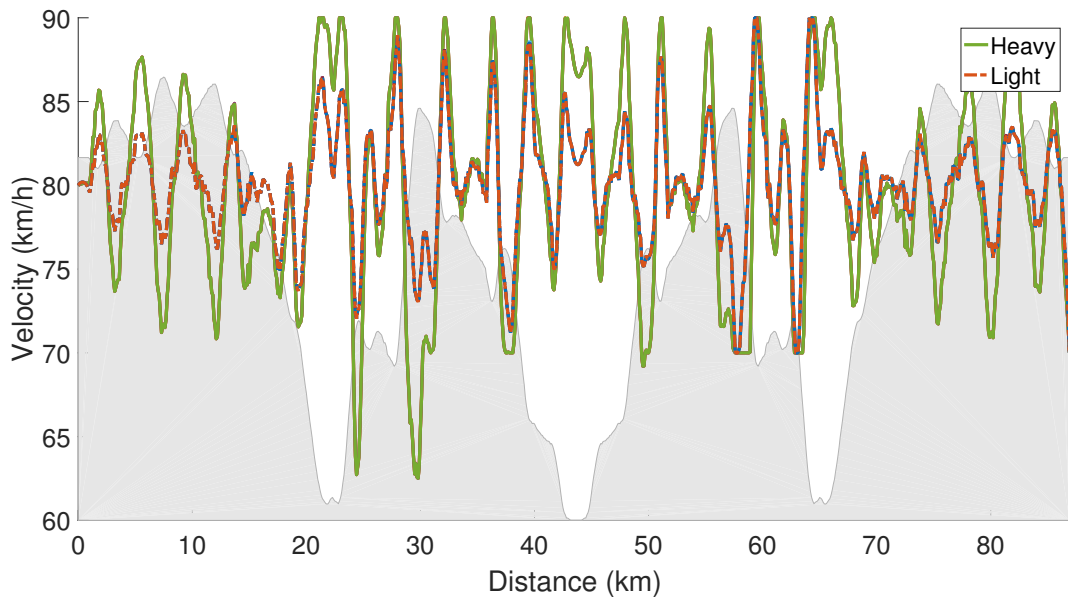


Figure C.1: Comparison of the velocity profiles between a light (18.5 t) 4-vehicle platoon and a heavy (41.8 t) 4-vehicle platoon, for all the members of the platoon.

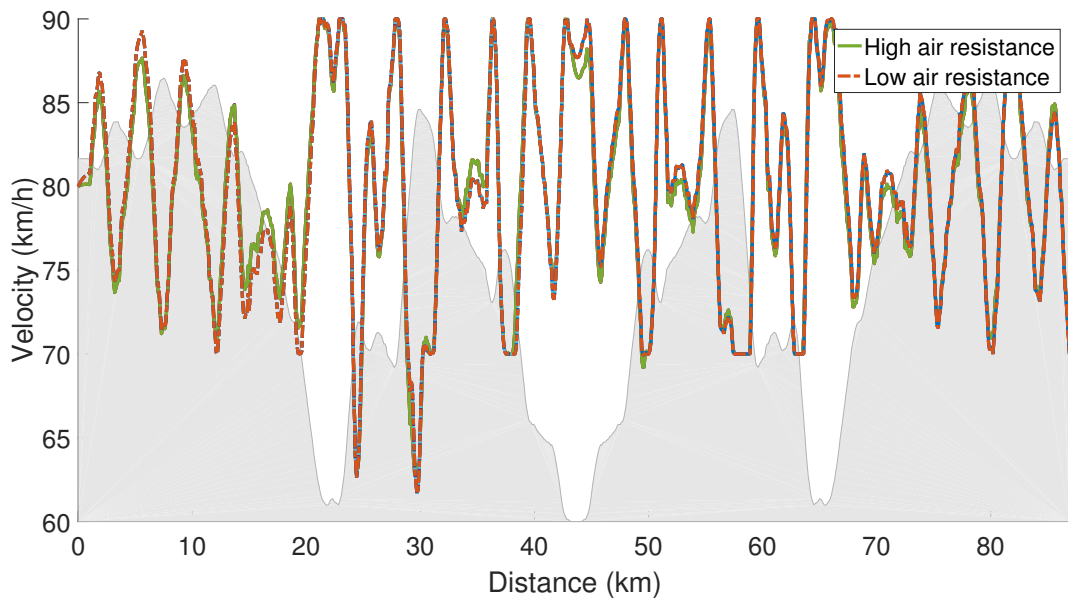


Figure C.2: Comparison of the velocity profiles between a 4-vehicle platoon with low air resistance ($c_d = 0.3$) and 4-vehicle platoon ($c_d = 0.6$), for all the members of the platoon.